

## CHAPTER VII

### DATA ANALYSIS AND RESULTS FOR SUNLIT ATRIA

#### 7.1 SUNLIGHT ILLUMINANCE LEVELS IN ATRIA

##### 7.1.1 Review of Direct Beam Sunlight

As discussed in Chapter 5, the illuminance measurements with the artificial sun under night sky recorded illuminances only from the sun. This is the same approach as in common building energy analysis in which the direct beam solar radiation and diffuse sky radiation are separately measured and/or calculated, then added later. This is because the direct beam radiation and diffuse sky radiation behave differently from each other. Since, the direct beam sunlight, which is the topic of this chapter, is the visible spectrum band (400 to 700 nm wavelengths) of the solar radiation, it might be helpful to briefly discuss solar radiation.

The solar radiation recorded at the earth's surface on a horizontal plane consists of two components, the direct (sun) component and the diffuse (sky and cloud) component. The direct component of solar radiation is called "direct beam radiation" and defined as "solar radiation received from the sun without change of direction". The diffuse component of solar radiation is called "diffuse sky radiation" and defined as "solar radiation received from the sun after its direction has been changed by reflection and scattering by the atmosphere" (Duffie and Beckman 1974, p. 8). As the direct solar beam traverses the atmosphere, it becomes diminished, while an increase in the amount of reflected or diffuse radiation occurs. The sun's rays are absorbed selectively in the atmosphere, the ultra violet by nitrogen, oxygen, and ozone, and the infrared by carbon dioxide and water vapor (Griffiths 1976, p. 15).

Another important factor which affects the intensity of direct beam radiation on a horizontal surface is the sun altitude angle. As the sun altitude angle decreases, the rays must traverse more of the atmosphere (optical air mass), so that depletion increases. On completely clear days, the direct-to-diffuse ratio ( $D/d$ ) is almost zero at sunrise and sunset, but increases to about 1.5 with the sun  $10^\circ$  above the horizon and to about 4 when the sun is at  $40^\circ$  altitude or greater (Griffiths 1976, p. 11). For outdoor horizontal illuminance levels, the annual average global-to-diffuse ratios ( $G/d$ ) were prepared for selected cities in the United States by Robbins and Hunter (1983). With a  $G/d = 6.0$ , the  $D/d$  becomes 5.0.

### 7.1.2 Sunlight Illuminance Levels and Distributions without Canopy

The impacts of atrium well configuration on interior sunlight illuminance levels were examined with Base Case Sunlight Illuminance Ratio (BCSIR) values of uncovered atria which had four different Well Index values (0.6, 1.2, 1.8 and 2.4). The artificial sun was located at nine different altitude angles representing the noon sun altitudes on three different days of the year in three different geographic locations (Houston, TX; Oklahoma City, OK; and Minneapolis, MN). More detailed discussions on the geographic locations, sun altitude angles, and instrument setup can be found in Chapters 4 and 5.

First of all, the impacts of atrium well configuration on interior sunlight illuminance levels were roughly examined with the minimum, maximum, average, and standard deviations of the BCSIR values. Tables 7.1 through 7.3 summarize the statistics of the BCSIR values for the three geographic locations, respectively. Then, the values are plotted in Figures 7.1 through 7.3.

TABLE 7.1  
Statistics of Base Case SIR Values for Houston, TX

Well Index	Day	Sun Alt.	Min. [%]	Max. [%]	Ave. [%]	SD [%]
0.6	06/21	84.0°	102.0	106.0	103.4	1.6
	09/21	60.3°	2.9	105.0	60.14	53.2
	12/21	37.1°	4.0	102.1	19.5	36.5
1.2	06/21	84.0°	65.0	103.3	97.0	14.1
	09/21	60.3°	4.4	106.4	49.8	52.1
	12/21	37.1°	5.4	10.9	7.8	1.8
1.8	06/21	84.0°	58.1	117.5	99.9	19.4
	09/21	60.3°	4.9	86.7	20.6	29.4
	12/21	37.1°	2.5	6.1	4.7	1.3
2.4	06/21	84.0°	4.5	114.1	64.3	55.6
	09/21	60.3°	5.8	16.6	8.7	4.1
	12/21	37.1°	1.4	4.7	3.6	1.1

TABLE 7.2  
 Statistics of Base Case SIR Values for Oklahoma City, OK

Well Index	Day	Sun Alt.	Min. [%]	Max. [%]	Ave. [%]	SD [%]
0.6	06/21	78.2°	7.4	107.4	90.4	36.7
	09/21	54.5°	2.8	118.7	65.9	58.5
	12/21	31.3°	4.8	9.6	7.9	1.5
1.2	06/21	78.2°	3.0	114.3	63.5	55.7
	09/21	54.5°	5.4	100.9	19.9	35.7
	12/21	31.3°	5.8	9.8	7.3	1.5
1.8	06/21	78.2°	3.7	121.3	66.7	58.3
	09/21	54.5°	5.4	10.3	7.9	2.0
	12/21	31.3°	2.5	3.7	3.1	0.5
2.4	06/21	78.2°	3.5	109.4	55.4	48.0
	09/21	54.5°	2.6	5.9	4.5	1.2
	12/21	31.3°	1.1	1.7	1.5	0.2

TABLE 7.3  
 Statistics of Base Case SIR Values for Minneapolis, MN

Well Index	Day	Sun Alt.	Min. [%]	Max. [%]	Ave. [%]	SD [%]
0.6	06/21	68.9°	1.8	103.4	87.2	37.7
	09/21	45.2°	2.2	113.2	49.2	56.7
	12/21	22.0°	6.7	27.6	16.4	9.5
1.2	06/21	68.9°	3.6	107.5	61.2	53.7
	09/21	45.2°	5.8	20.3	11.4	5.3
	12/21	22.0°	1.9	6.0	4.8	1.4
1.8	06/21	68.9°	3.9	106.0	47.8	53.3
	09/21	45.2°	4.7	13.3	8.3	3.6
	12/21	22.0°	1.5	3.0	2.3	0.6
2.4	06/21	68.9°	4.6	22.1	8.7	6.1
	09/21	45.2°	1.4	3.0	2.4	0.6
	12/21	22.0°	1.0	2.8	1.4	0.7

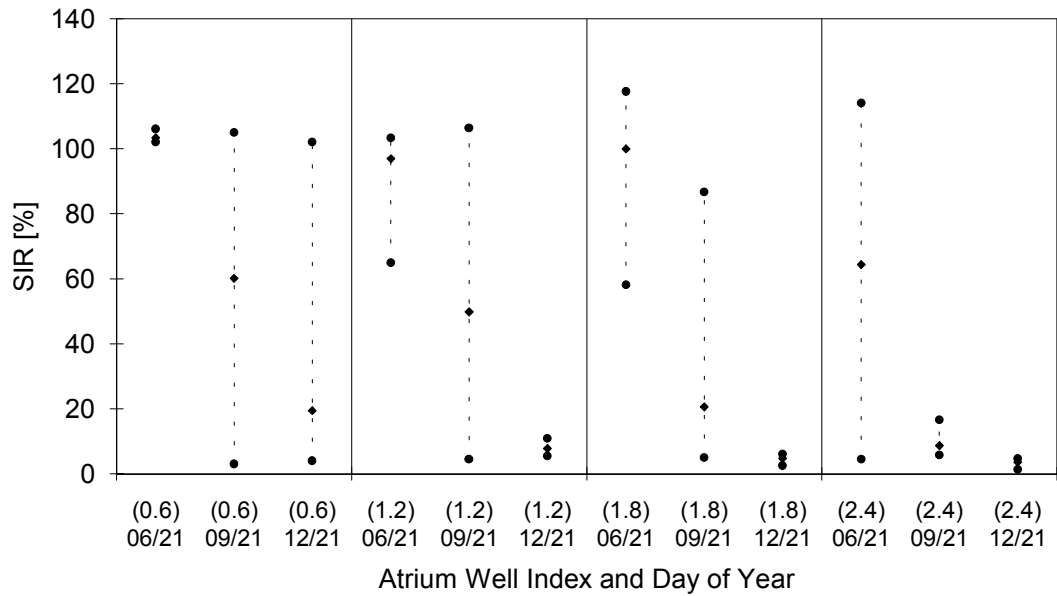


Figure 7.1 Minimum, Maximum, and Average SIR Values without Canopy at Three Solar Noon Hours in Houston, TX

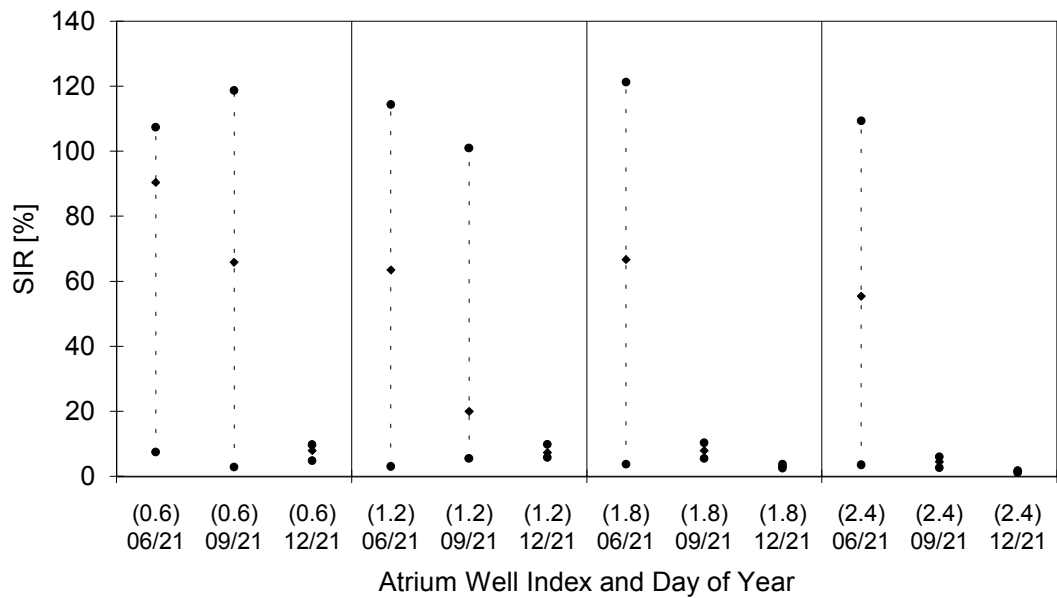


Figure 7.2 Minimum, Maximum, and Average SIR Values without Canopy at Three Solar Noon Hours in Oklahoma City, OK

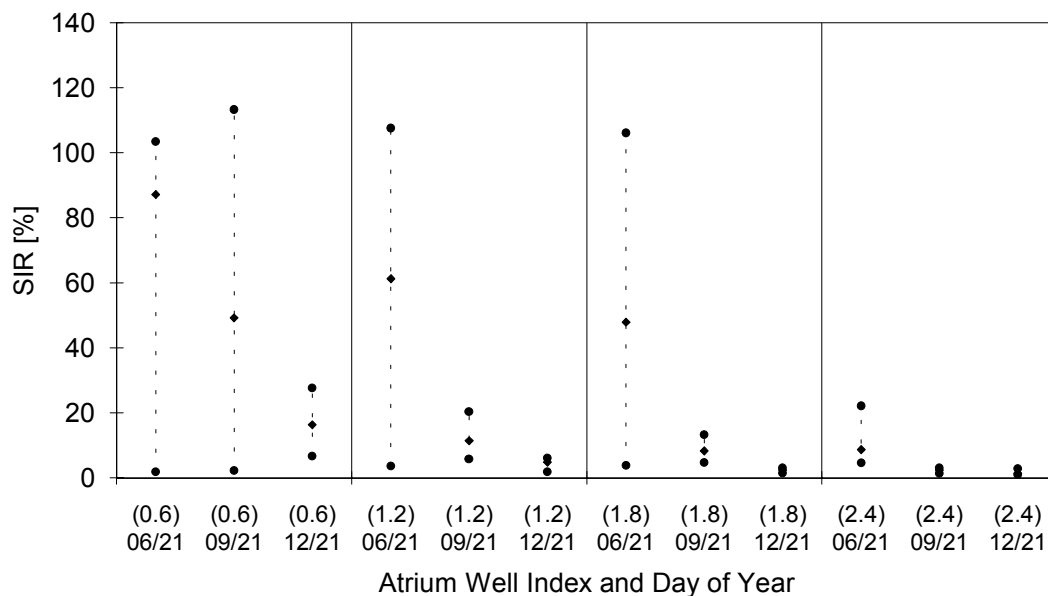


Figure 7.3 Minimum, Maximum, and Average SIR Values without Canopy at Three Solar Noon Hours in Minneapolis, MN

As indicated in the above tables and figures, the SIR values showed totally different features from the DF values which were discussed in Chapter 6. In the case of Base Case DF values, those at the center floor position were always higher than those at the other floor positions. Furthermore, the maximum DF difference between the center floor position and the average of remaining floor positions did not exceed 12 % (see Table 6.4).

However, in the case of Base Case SIR values, the great standard deviation values at certain combinations of the sun altitude angles and the WI values imply large differences in SIR values among the floor positions. In other words, they imply that the direct sunlight illuminated partial floor areas, so that the floor positions exposed to the sun and those at shaded floor positions received light flux with substantially different intensities. In real situations, since the direct beam sunlight illuminance is much higher than diffuse daylight illuminance, greatly uneven illuminance distributions are expected in these cases. On the contrary, at certain conditions, the SIR differences were very small. In these cases, the small values of standard deviations imply that most of the floor positions were either exposed to the sun or shaded by the atrium structure.

When the minimum and maximum (mostly maximum) SIR values were examined, it was shown that some SIR values exceeded 100 % especially at high sun altitude angles. This was because the illuminance measured at the floor positions which were fully exposed to the sunlight consisted of both the Direct Sun Component (DSC) and the Internally Reflected Component (IRC).

The SIR values at the seven different floor positions are presented in Tables 7.4 through 7.6 for the three geographic locations. The BCSIR values at the seven floor positions were analyzed to examine the spatial distributions of sunlight illuminances on the atrium floor level. Figures 7.4 through 7.6 show the plots of SIR values.

TABLE 7.4  
Base Case SIR Values at Seven Floor Positions for Houston, TX

Well Index	Day	Sun Alt.	SIR [%]						
			1	2	3	4	5	6	7
0.6	06/21	84.0°	102.0	102.0	106.0	103.0	104.0	102.0	105.0
	09/21	60.3°	2.9	101.1	102.0	3.6	103.0	3.4	105.0
	12/21	37.1°	4.0	10.2	102.0	4.5	4.8	5.1	5.6
1.2	06/21	84.0°	65.0	102.1	102.5	101.8	102.9	101.5	103.3
	09/21	60.3°	4.4	16.4	104.0	5.8	105.8	6.0	106.4
	12/21	37.1°	9.6	10.9	5.4	6.9	7.2	7.3	7.6
1.8	06/21	84.0°	58.1	101.9	103.0	101.5	117.5	101.3	110.1
	09/21	60.3°	4.9	11.6	86.7	7.2	13.0	6.5	14.2
	12/21	37.1°	6.1	5.0	2.5	5.8	3.9	5.8	4.0
2.4	06/21	84.0°	5.4	100.7	107.8	4.5	112.4	5.0	114.1
	09/21	60.3°	16.6	6.5	12.2	5.8	7.0	5.8	7.3
	12/21	37.1°	4.0	3.9	1.4	4.5	3.0	4.7	4.0

TABLE 7.5  
Base Case SIR Values at Seven Floor Positions for Oklahoma City, OK

Well Index	Day	Sun Alt.	SIR [%]						
			1	2	3	4	5	6	7
0.6	06/21	78.2°	7.4	107.4	101.4	101.4	105.8	102.2	107.4
	09/21	54.5°	2.8	103.7	111.0	3.9	118.7	4.2	117.2
	12/21	31.3°	4.8	7.6	9.6	8.0	8.7	8.5	8.2
1.2	06/21	78.2°	3	105.5	102.8	4.4	114.3	5.0	109.7
	09/21	54.5°	5.4	7.2	100.9	6.0	6.9	5.9	7.3
	12/21	31.3°	8.8	9.8	5.8	6.3	7.1	6.4	7.0
1.8	06/21	78.2°	3.7	121.3	102.2	5.3	118.9	5.2	110.6
	09/21	54.5°	5.4	7.3	10.3	6.3	9.8	6.2	9.7
	12/21	31.3°	3.6	3.3	2.5	3.7	2.7	3.5	2.6
2.4	06/21	78.2°	3.5	50.9	102.0	10.9	100.6	10.5	109.4
	09/21	54.5°	4.1	5.9	2.6	5.4	3.7	5.5	4.0
	12/21	31.3°	1.4	1.3	1.1	1.7	1.4	1.7	1.6

TABLE 7.6  
Base Case SIR Values at Seven Floor Positions for Minneapolis, MN

Well Index	Day	Sun Alt.	SIR [%]						
			1	2	3	4	5	6	7
0.6	06/21	68.9°	1.8	100.9	101.4	101.2	103.4	100.1	101.8
	09/21	45.2°	2.2	5.5	106.4	3.6	109.7	3.9	113.2
	12/21	22.0°	8.6	9.6	27.6	6.7	27.2	10.4	24.5
1.2	06/21	68.9°	3.6	107.5	103.0	4.0	105.1	4.0	101.5
	09/21	45.2°	8.5	9.0	20.3	5.8	14.0	6.7	15.5
	12/21	22.0°	4.4	5.5	1.9	5.7	5.4	6.0	5.0
1.8	06/21	68.9°	3.9	6.3	103.0	4.7	106.0	5.4	101.1
	09/21	45.2°	4.8	13.3	4.7	11.7	6.1	11.4	6.4
	12/21	22.0°	1.5	3.0	1.9	2.9	2.2	3.0	1.7
2.4	06/21	68.9°	7.2	6.1	22.1	4.9	8.3	4.6	7.7
	09/21	45.2°	2.5	3.0	1.4	2.9	2.1	2.8	2.4
	12/21	22.0°	1.0	2.8	1.9	1.0	1.0	1.4	1.0

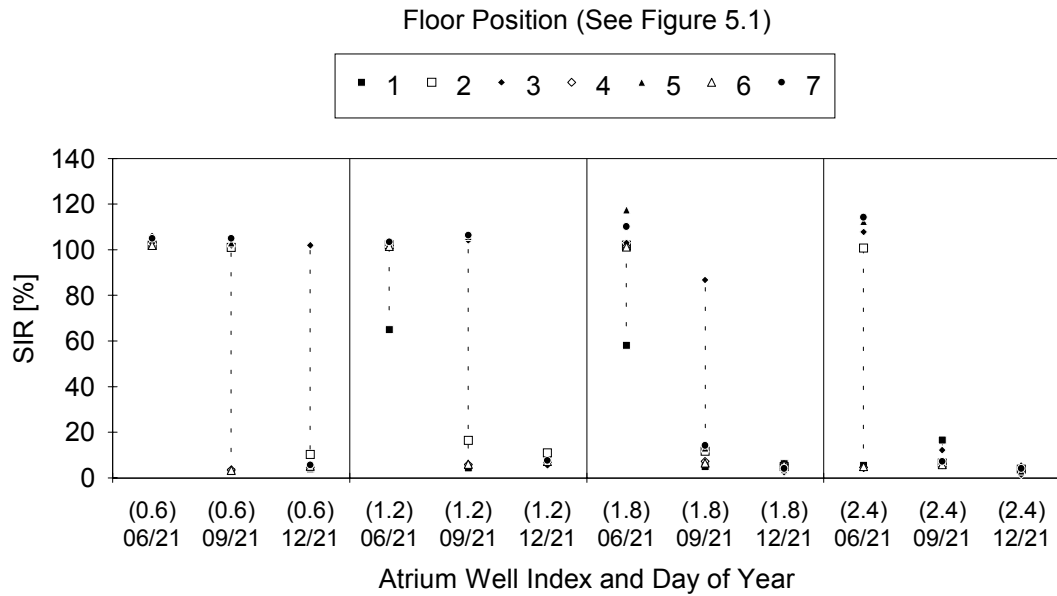


Figure 7.4 Base Case SIR Values at Three Solar Noon Hours in Houston, TX

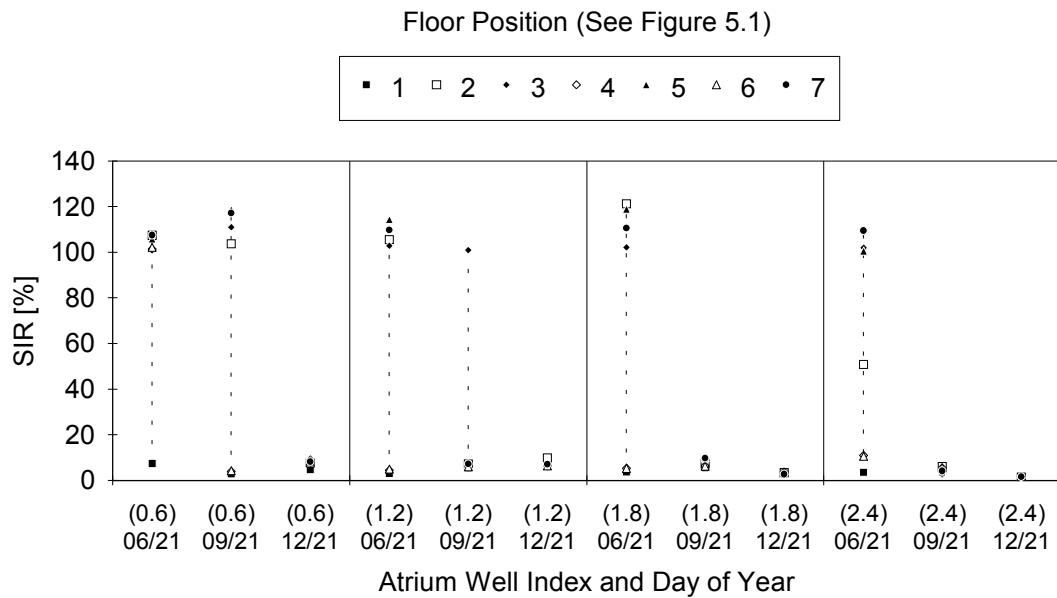


Figure 7.5 Base Case SIR Values at Three Solar Noon Hours in Oklahoma City, OK



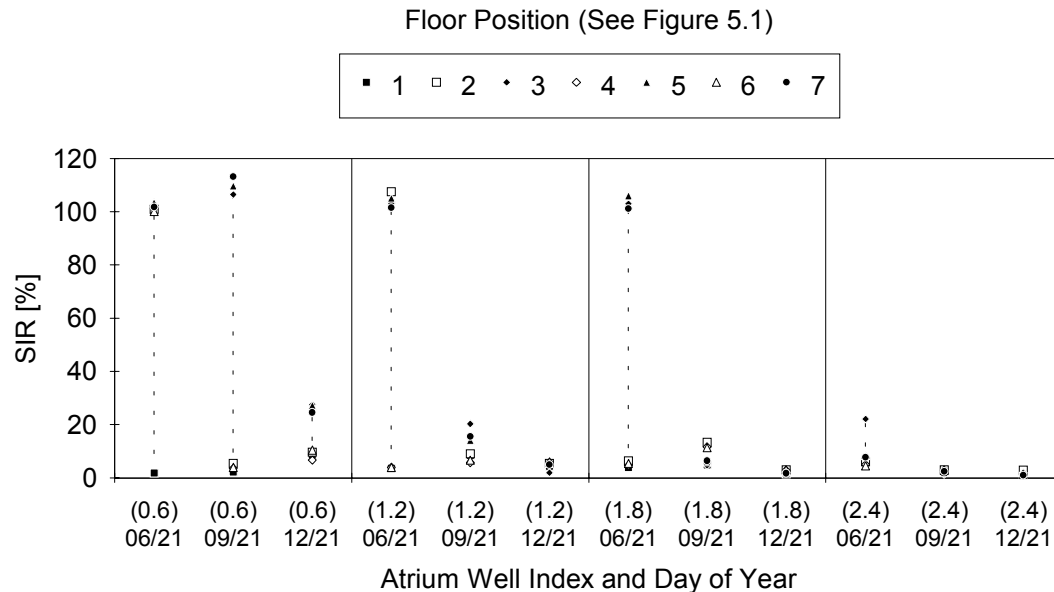


Figure 7.6 Base Case SIR Values at Three Solar Noon Hours in Minneapolis, MN

In the above figures, notable features of the BCSIR values were the polarized distributions. First, when the sunlight illuminated certain parts of the floor area, the SIR values at certain groups of the seven floor positions polarized toward the top and the bottom. Second, when most of the floor area was exposed to the sunlight, all of the seven SIR values polarized to the top, and vice versa. Furthermore, with SIR values smaller than 100 % but still much greater than the fully shaded SIR values, some photometric sensors were evidently partially shaded. Such a case was observed at the center floor position at WI of 2.4 (atrium A8) on June 21 in Oklahoma City shown in Figure 7.5. As discussed in Chapter 5, the previous Tables 5.1 through 5.3 listed floor positions exposed to the artificial sun, and if a photometric sensor which must be in shadow area recorded a high illuminance level, the photometric sensor was visually observed. From the visual observations, it was found that some photometric sensors were marginally located on the boundary between the shadow area and the fully exposed area.

Another interesting feature observed during the measurement procedure was that the light reflected from the atrium well surfaces did not uniformly illuminate the entire floor area. Figure 7.7 shows a photographic image taken during the measurement with WI of 1.2 (atrium A4) on September 21 for Houston. As shown in the figure, the photometric

sensors at the floor positions 3, 5, and 7 were fully exposed to the sunlight and it was easy to imagine that those photometric sensors also received light reflected from the north wall surface. In addition, note the bright band on the center floor area, which was created by high-intense light flux due to specular reflection at a window area, marginally covered the photometric sensor located on the floor position 2. As presented in Table 5.4, the SIR value at that position was 16.4 %, while the average SIR value of the floor positions 1, 4, and 6 were 5.4 %.

Furthermore, Figure 7.7 demonstrates the importance of accurate positioning of photometric sensors in terms of the elevation and horizontal locations in scale models especially for sunlight illuminance measurement. The line "A" drawn on the photo indicates the shadow line which lies on the wooden holder just before the photometric sensors 5 and 7. Meanwhile, the line "B" indicates the shadow line which lies on the floor surface just after the two photometric sensors. If the two sensors were moved toward the south wall or the elevations were lowered from the current position, resulting illuminance levels should be much lower than the actual recorded illuminances. As previously shown in Table 5.1, the two sensors were to be fully exposed to the artificial sun. Figure 7.8 shows the SIR values plotted for the seven floor positions.

Therefore, it can be concluded from this initial analysis that the major factors which determine the sunlight illuminance levels at a floor position include:

- 1) the geometric relationship between the sun and the atrium well structure which determines the proportions of shadow areas and exposed areas on interior surfaces including walls and floor,
- 2) the geometric relationships between the floor positions and atrium well surfaces which determine the Configuration Factors (CF) of high-luminance interior surfaces fully exposed to the sun,
- 3) the reflectances of wall surfaces which determine the intensity of Internally Reflected Component (IRC) of sunlight,
- 4) and the locations and areas of specular glazed windows which determine the intensity as well as the direction of specularly reflected light.

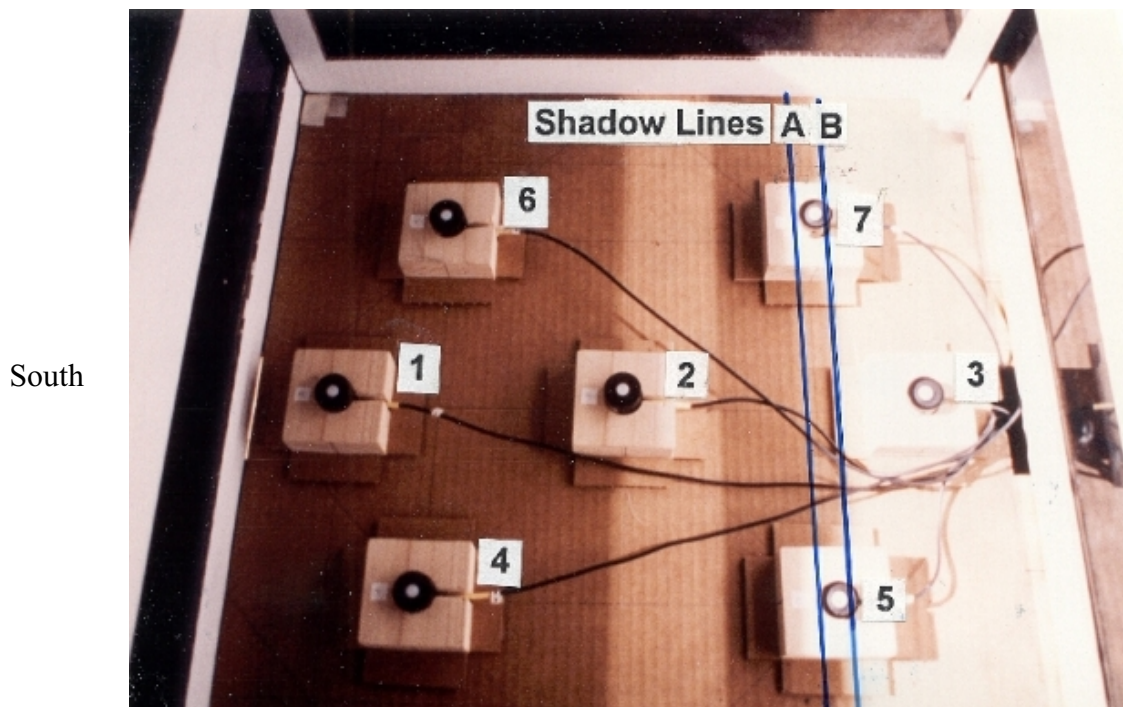


Figure 7.7 Photo of Shaded and Fully Exposed Floor Positions at WI = 1.2 (Atrium A4) without Canopy (Sun Alt. = 60.3°, 9/ 21, Houston, TX)

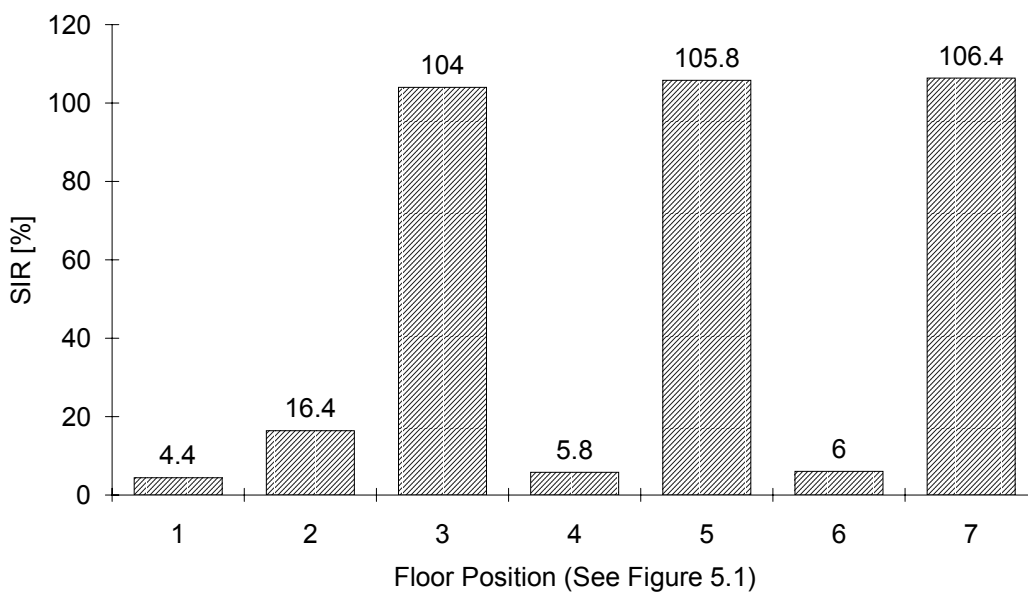


Figure 7.8 Base Case SIR Values at Seven Floor Positions (WI = 1.2, Sun Alt. = 60.3°, 9/21, Houston, TX)

### 7.1.3 Sunlight Illuminance Levels and Distributions with Canopies

The effects of canopy configurations on noon sunlight illuminance levels at the seven floor positions were examined with a total of 17 canopy configurations which were previously shown in Figure 4.12. For this test, four different atria with WI values of 0.6, 1.2, 1.8 and 2.4 were assumed at different seasons for three different geographic locations.

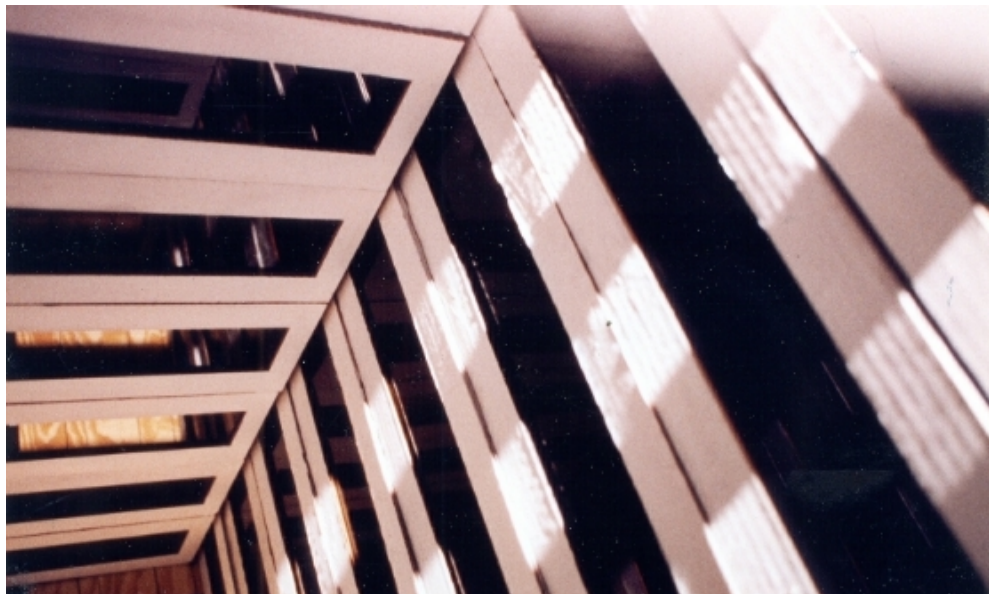
In dealing with sunlight illuminances with canopies, the sunlight illuminances at each floor position might be less meaningful, because, as demonstrated in the previous sections, a small geometric deviation from the sunlit area causes great differences in the measured illuminance. Such cases were frequently observed during the measurement procedure. Even a vague patch of linear shadow cast on a specific photometric sensor by a linear structural member resulted in substantial reduction in the measured illuminance level. This problem is well demonstrated in Figure 7.9 which shows the photo of sunlighting condition in a 2-story atrium (WI = 0.6) at sun altitude angle of  $84.0^\circ$  (solar noon on June 21 in Houston, TX). Note the linear shadows on the floor area cast by the structural members of the pyramid skylight. If the linear shadows happened to cover all of the seven photometric sensors on the floor positions, all of the measured illuminance levels would be very low, even though most of the floor area is exposed to the sun. Another example is shown in Figure 7.10, which shows the sunlit and shadow area in the same atrium with the sawtooth canopy with  $15^\circ$  sloping apertures at sun altitude angle of  $45.2^\circ$  (solar noon on September 21 in Minneapolis, MN). Note the photometric sensor located closest to the shadow cast by the second solid panel from the front. Even though the photometric location is the boundary line between the sunlight and shadow, the measured high illuminance cannot explain the average condition around the position.

In addition, even though the parameterized canopy scale models involved in this study can characterize the lighting performances of same types of canopy in real situations, it is impossible to construct scale models which match all possible combinations of real world canopy features. Therefore, instead of dealing with the illuminance distributions on the floor positions, the minimum, maximum, average, and standard deviations of the Sunlight Illuminance Ratio (SIR) values were analyzed to understand the characteristic performances of the canopy systems. In the current analysis, two extreme seasons (Houston summer and Minneapolis winter) and one intermediate season (Oklahoma City fall) were involved. With these seasons and geographic locations, the given sun altitude angles were  $84.0^\circ$ ,  $54.5^\circ$ , and  $22.0^\circ$ .



South

Figure 7.9 Photo of Linear Shadows Cast by Linear Structural Members  
(Atrium A2, Sun Alt. =  $84.0^\circ$ , 6/21, Houston, TX)



South

Figure 7.10 Photo of Shadows Cast by Sawtooth Canopy with  $15^\circ$  Sloping Apertures  
(Atrium A2, Sun Alt. =  $45.2^\circ$ , 9/21, Minneapolis, MN)

Tables 7.7 through 7.10 present the statistics of SIR values at solar noon on June 21 in Houston, TX. Figures 7.11 through 7.14 show them in graphic formats with the previously discussed Base Case SIR (BCSIR) values at the first columns. As indicated in the tables and figures, different type canopy systems resulted in different average SIR values and standard deviations.

The sawtooth canopies with south-facing vertical apertures (No. 04S and 08S) showed low SIR values at  $WI = 0.6$  (atrium A2) and  $WI = 1.2$  (atrium A4), but showed increased SIR values at  $WI = 1.8$  (atrium A6) and  $WI = 2.4$  (atrium A8). The low average SIR values and the small standard deviations for these canopies at the two lower WI values shown in Tables 7.7 and 7.8 indicate that most of the photometric sensors were within shadow area. However, much higher average SIR values and the larger standard deviations at the two higher WI values imply that several sensors were exposed to the direct sunlight. This is the characteristic performance of sawtooth canopies with vertical apertures at high sun altitude angles, because the large areas of solid panels block most of the direct beam sunlight and the south-facing apertures admit only fractions of incoming beam sunlight. However, the sawtooth canopies with north-facing vertical apertures (No. 04N, 08N, and 12N) recorded consistently low SIR values. With these canopy configurations and the orientation, the direct beam sunlight from the south hit the sawtooth panels and is interreflected between the inside and outside surfaces of contiguous panels, so that only diffuse light can be admitted into the atrium space.

Meanwhile, the sawtooth canopies with sloping apertures (No. 13S, 13N, 16S, and 16N) caused higher SIR values and larger standard deviations than those of vertical-opening sawtooth canopies throughout the four WI values, except for the canopy 16N at  $WI = 1.2$ . With these canopy configurations at this high sun angle, it is easy to imagine that the large horizontally projected aperture areas and the solid panels would create repetitive patterns of large bands of fully exposed and shaded areas on the atrium floor, which would cause repetitive fluctuations in illuminance levels proportional to the number of units and pitches of the open and opaque areas.

In general, the flat horizontal skylight (No. 19) and the pyramid skylight (No. 27) with tinted transparent glazing also caused high SIR values with large standard deviations at all WI values. Again, the waffle skylights also resulted in high SIR values with large standard deviations.

A notable feature at this high sun altitude angle was the consistent performances of the skylight systems with translucent glazing (No. 20 and 28). The SIR values of these canopies were always low and the standard deviations were also very low. Even though

the average Hemispherical Transmittance (HT) measured under diffuse skies was 35.8 % (see Figure 5.27), the SIR values ranged from 2.8 % to 10.5 % with the flat horizontal skylight (No. 20) and from 1.9 % to 9.5 % with the pyramid skylight (No. 28). When the SIR values of the two skylights at different WI values were examined, it was found that the SIR values decreased with higher WI values. This is the characteristic performance of a skylight system with translucent glazing material. Since the beam sunlight is totally diffused when it is transmitted through the glazing material, the skylight performs like a diffuse sky. Therefore, the decreasing Configuration Factor (CF) of the opening area seen from floor positions with increasing WI value causes lower SIR values.

With this initial assessment on the characteristic performance of canopy systems at this high sun altitude angle, it was temporarily concluded that choosing sawtooth canopies with north-facing vertical apertures would be the safest way to keep atrium buildings from excessive sunlight penetration and instantaneous solar heat gain in this hot climatic zone. If sun sparkle is desired as a design element, sawtooth canopies with south-facing vertical apertures might be the choice. On the other hand, if a pyramid or space-frame structure is desired as a monumental design feature, covering it with translucent glazing material might be the most effective way concerning thermal conditioning load. However, this temporary conclusions were only based on the results with this high sun altitude angle. More assessments with lower sun angles are required to select optimum canopy configurations in this predominantly hot climate.

TABLE 7.7  
 Statistics of SIR Values at WI = 0.6 with 17 Canopy Configurations  
 at Sun Alt. = 84.0° (Solar Noon, 6/21, Houston, TX)

Canopy Code *	Min [%]	Max [%]	Ave [%]	SD [%]	Canopy Code *	Min [%]	Max [%]	Ave [%]	SD [%]
04S	4.7	7.6	6.3	1.0	04N	2.8	5.3	4.0	0.9
08S	7.4	43.5	13.7	13.2	08N	5.5	8.5	6.9	1.0
12S	7.1	9.1	8.0	0.6	12N	5.5	7.7	6.6	0.7
13S	3.0	100.0	30.4	46.4	13N	2.7	100.3	72.7	46.3
16S	4.8	97.7	18.4	35.0	16N	3.9	43.3	13.7	16.0
19	23.6	46.6	36.3	8.4					
20	9.9	11.8	10.5	0.6					
27	20.3	44.8	38.4	8.9					
28	8.3	11.2	9.5	1.0					
33	39.7	100.8	65.4	25.4					
34	10.6	101.0	64.0	31.8					
36	9.8	101.8	66.5	35.8					

\* See Table 4.8 for Canopy Code (S = South, N = North)

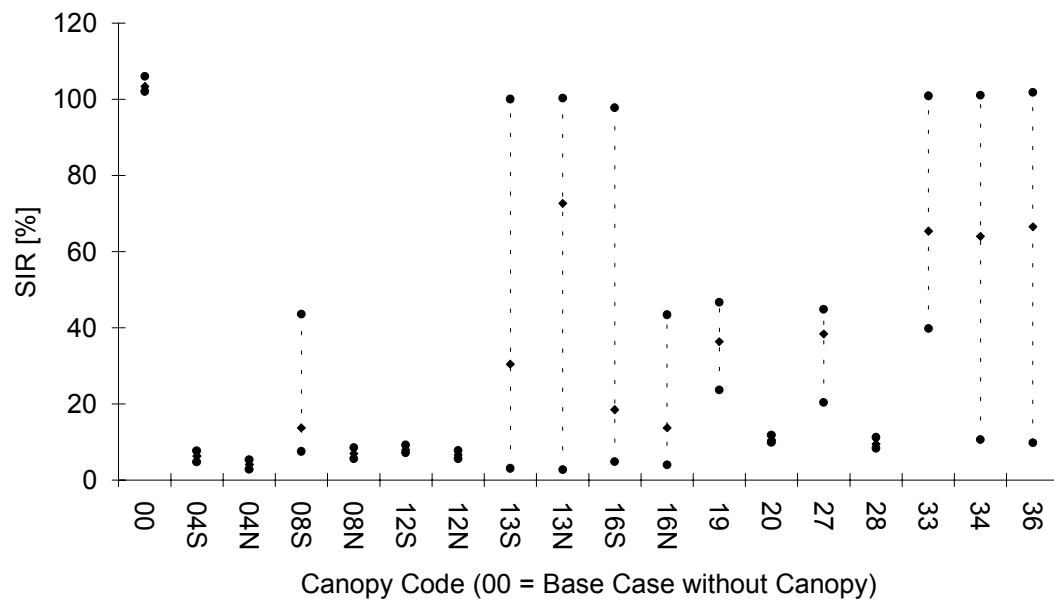


Figure 7.11 Minimum, Maximum, and Average SIR Values at WI = 0.6 with Canopies (Solar Noon, 6/21, Houston, TX, Sun Alt. = 84.0°)



TABLE 7.8  
 Statistics of SIR Values at WI = 1.2 with 17 Canopy Configurations  
 at Sun Alt. = 84.0° (Solar Noon, 6/21, Houston, TX)

Canopy Code *	Min [%]	Max [%]	Ave [%]	SD [%]	Canopy Code *	Min [%]	Max [%]	Ave [%]	SD [%]
04S	3.5	4.9	4.2	0.5	04N	1.5	2.7	2.0	0.4
08S	4.8	5.8	5.3	0.5	08N	3.1	4.3	3.9	0.4
12S	4.7	14.6	8.0	4.3	12N	3.4	4.4	3.8	0.4
13S	2.5	99.7	44.7	50.8	13N	2.4	113.2	35.0	43.9
16S	3.3	75.8	24.6	34.9	16N	2.3	3.0	2.6	0.3
19	2.2	49.9	33.8	16.0					
20	5.8	6.5	6.2	0.3					
27	2.4	46.0	34.2	16.4					
28	4.8	5.6	5.2	0.3					
33	3.8	102.8	85.1	48.0					
34	3.2	100.4	62.9	30.1					
36	2.2	53.1	40.6	17.6					

\* See Table 4.8 for Canopy Code (S = South, N = North)

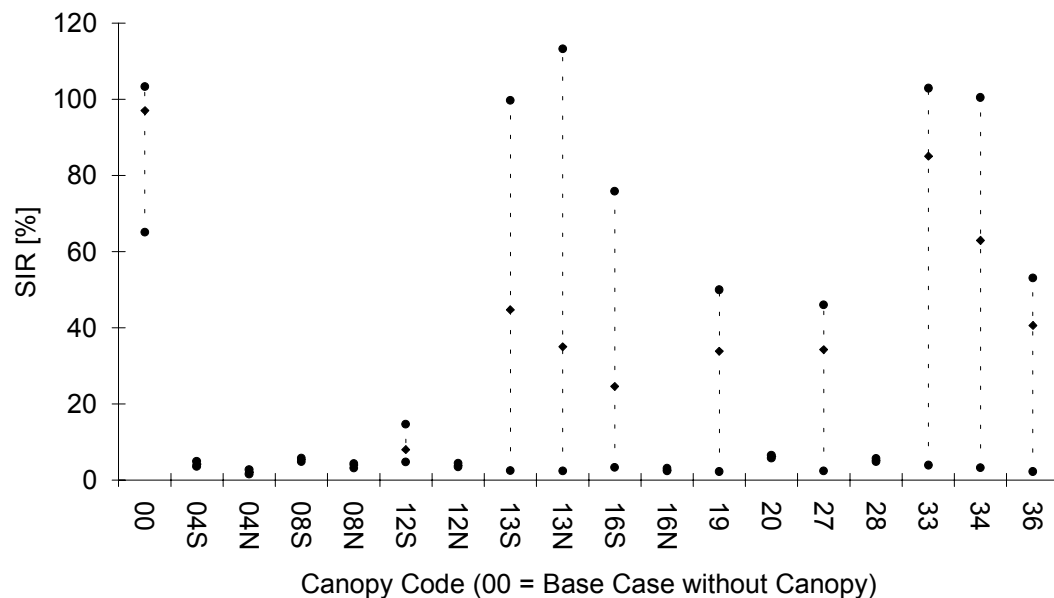


Figure 7.12 Minimum, Maximum, and Average SIR Values at WI = 1.2 with Canopies (Solar Noon, 6/21, Houston, TX, Sun Alt. = 84.0°)

TABLE 7.9  
 Statistics of SIR Values at WI = 1.8 with 17 Canopy Configurations  
 at Sun Alt. = 84.0° (Solar Noon, 6/21, Houston, TX)

Canopy Code *	Min [%]	Max [%]	Ave [%]	SD [%]	Canopy Code *	Min [%]	Max [%]	Ave [%]	SD [%]
04S	1.2	45.0	23.7	20.5	04N	0.2	2.0	1.5	0.6
08S	2.1	82.5	31.7	36.4	08N	0.2	3.2	2.2	1.0
12S	2.1	44.1	18.3	16.0	12N	0.2	2.9	2.2	1.0
13S	47.4	102.6	77.1	24.1	13N	0.7	40.9	11.7	16.0
16S	5.2	97.0	24.7	33.6	16N	0.2	30.2	9.8	13.1
19	7.2	40.9	32.0	11.2					
20	1.6	4.6	3.7	1.1					
27	5.7	46.3	31.1	14.3					
28	1.2	3.9	3.1	0.9					
33	49.4	80.2	58.8	11.0					
34	33.4	55.2	41.2	8.0					
36	14.4	58.9	44.3	14.3					

\* See Table 4.8 for Canopy Code (S = South, N = North)

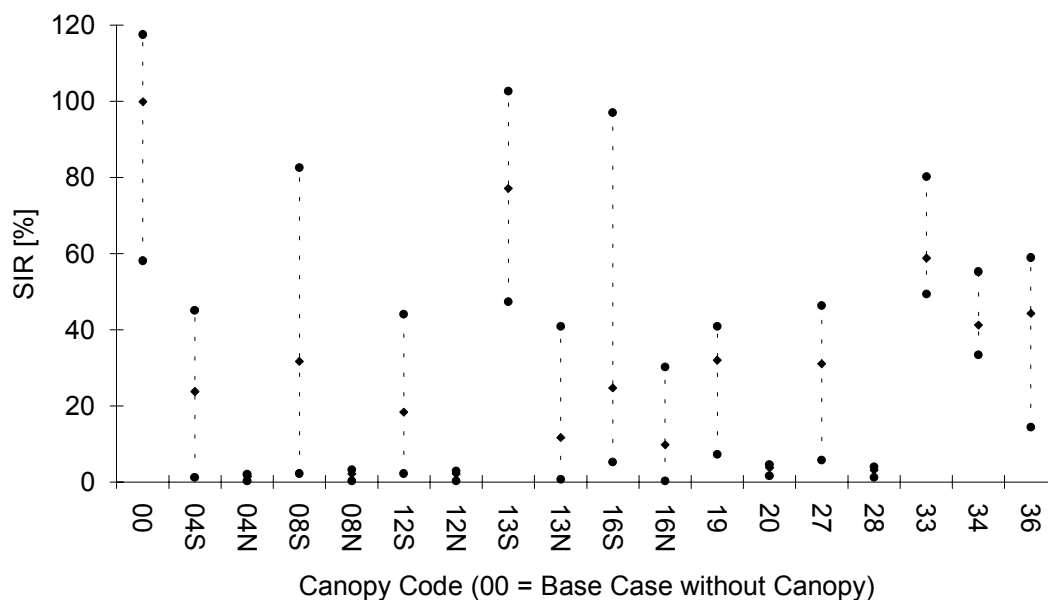


Figure 7.13 Minimum, Maximum, and Average SIR Values at WI = 1.8 with Canopies (Solar Noon, 6/21, Houston, TX, Sun Alt. = 84.0°)

TABLE 7.10  
 Statistics of SIR Values at WI = 2.4 with 17 Canopy Configurations  
 at Sun Alt. = 84.0° (Solar Noon, 6/21, Houston, TX)

Canopy Code *	Min [%]	Max [%]	Ave [%]	SD [%]	Canopy Code *	Min [%]	Max [%]	Ave [%]	SD [%]
04S	1.2	65	34.7	31.4	04N	0.3	1.8	1.0	0.5
08S	2.4	72.6	47	26.0	08N	0.2	2.2	1.4	0.8
12S	2.3	47.5	11.7	16.2	12N	0.3	2.3	1.6	0.8
13S	2.7	42.9	10.2	14.6	13N	3.2	102.1	53.8	48.0
16S	1.2	31.5	7.8	10.7	16N	1.5	85.4	20.1	31.7
19	2.0	42.2	22.2	19.2					
20	1.8	3.4	2.8	0.6					
27	2.7	92.2	50.4	34.9					
28	1.0	2.5	1.9	0.6					
33	5.2	96.1	62.6	40.3					
34	3.9	78.8	47.1	32.2					
36	2.8	47.1	28.1	18.9					

\* See Table 4.8 for Canopy Code (S = South, N = North)

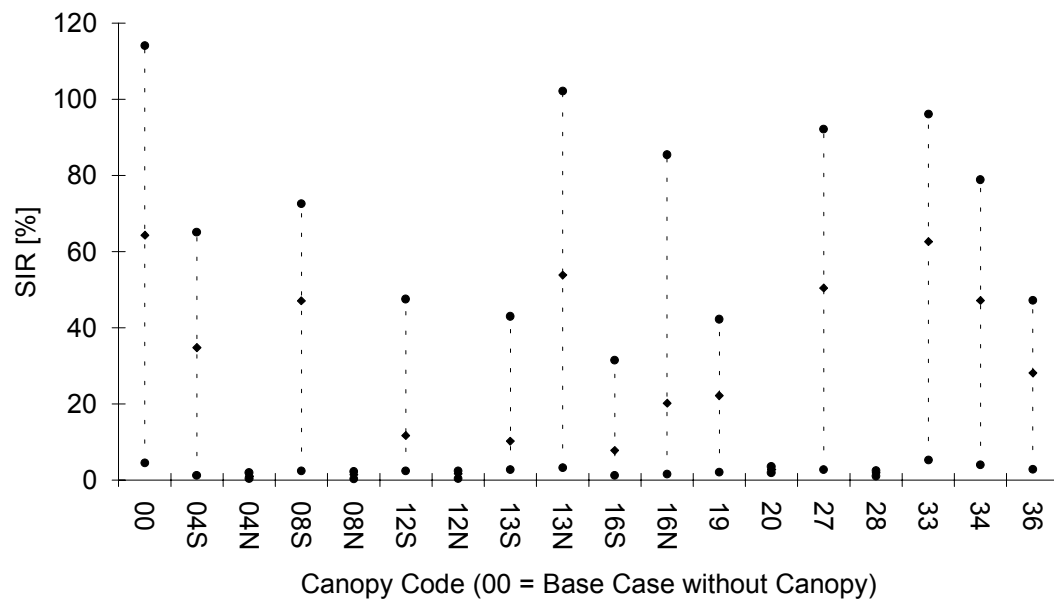


Figure 7.14 Minimum, Maximum, and Average SIR Values at WI = 2.4 with Canopies (Solar Noon, 6/21, Houston, TX, Sun Alt. = 84.0°)

Tables 7.11 through 7.14 and Figures 7.15 through 7.18 show the statistics of SIR values at solar noon hour (sun alt. =  $54.5^\circ$ ) on September 21 in Oklahoma City, OK. The overall picture at this condition was that, at WI values of 0.6 and 1.2, some canopies performed much differently from others, while at WI values of 1.8 and 2.4, not much differences were found and all of the canopies showed low SIR values.

A notable feature at this sun angle was the performance of sawtooth canopies with south-facing vertical apertures (No. 04S, 08S, and 12S). In the Houston case with the high sun, these canopies caused low SIR values at the two low WI values. However, now they resulted in much higher SIR values and large standard deviations at the two lower WI values.

The sawtooth canopies with north-facing vertical apertures (No. 04N, 08N, 12N) resulted in consistently low SIR values at all WI values. Meanwhile, the skylights with transparent glazing (No. 19 and 27) showed still relatively high SIR values and large standard deviations at WI = 0.6 and WI = 1.2.

Another notable feature was much reduced SIR values and standard deviations for waffle skylights at the two higher WI values. Especially, at WI = 1.2 (atrium A4), the average of the SIR values with the three waffle skylights (No. 33, 34, and 36) was about 14 % lower than that for the three sawtooth canopies (No. 04S, 08S, and 12S). Meanwhile, the average standard deviation for the three waffle skylights was about 30 % lower than that for the three sawtooth canopies. These phenomena indicate that at this specific WI value and the sun altitude angle, the south facing apertures admitted the direct beam sunlight on partial area of the floor, while the vertical structures of waffle skylights blocked most of the beam sunlight and reflected diffuse light toward the atrium space.

To help clarify the reverse performances of these two canopy types, simple 2-dimensional sun penetration diagrams are presented in Figure 7.19. As shown in the figure, the beam sunlight transmitted through the 2-unit and 4-unit sawtooth canopies illuminates the north wall and about 1/8th north portion of the floor area. The floor position 3 which was exposed to the sunlight (see also Table 5.3) recorded 109 % with the 2-unit sawtooth canopy and 108 % with the 4-unit sawtooth canopy (see the maximum SIR values in Table 7.12). On the contrary, the waffle skylight with 1.0 WWI transmits slender light beams mostly toward the north wall. Furthermore, the waffle skylight with 2.0 WWI completely blocks the beam sunlight.

Figure 7.19 also indicates that the WI of 1.2 was the marginal WI value at this sun altitude angle for the sun to illuminate any parts of the floor area. At a higher WI value, no floor area is expected to be exposed to the direct sun even without canopy.

TABLE 7.11  
 Statistics of SIR Values at WI = 0.6 with 17 Canopy Configurations  
 at Sun Alt. = 54.5° (Solar Noon, 9/21, Oklahoma City, OK)

Canopy Code *	Min [%]	Max [%]	Ave [%]	SD [%]	Canopy Code *	Min [%]	Max [%]	Ave [%]	SD [%]
04S	6.7	108.1	50.1	51.8	04N	0.9	2.7	1.8	0.6
08S	7.3	108.1	51.3	50.8	08N	2.6	4.7	4.0	0.7
12S	6.4	121.0	68.9	58.2	12N	3.4	4.7	4.1	0.5
13S	3.1	77.7	25.9	29.7	13N	2.3	70.6	17.7	25.4
16S	5.4	24.5	12.9	8.9	16N	2.6	3.7	3.2	0.4
19	0.8	43.1	19.3	19.1					
20	10.0	11.7	10.7	0.5					
27	0.8	46.6	20.2	19.9					
28	8.1	10.8	9.3	0.8					
33	6.7	48.8	19.2	17.7					
34	5.8	72.8	16.7	24.8					
36	1.4	6.1	4.0	1.7					

\* See Table 4.8 for Canopy Code (S = South, N = North)

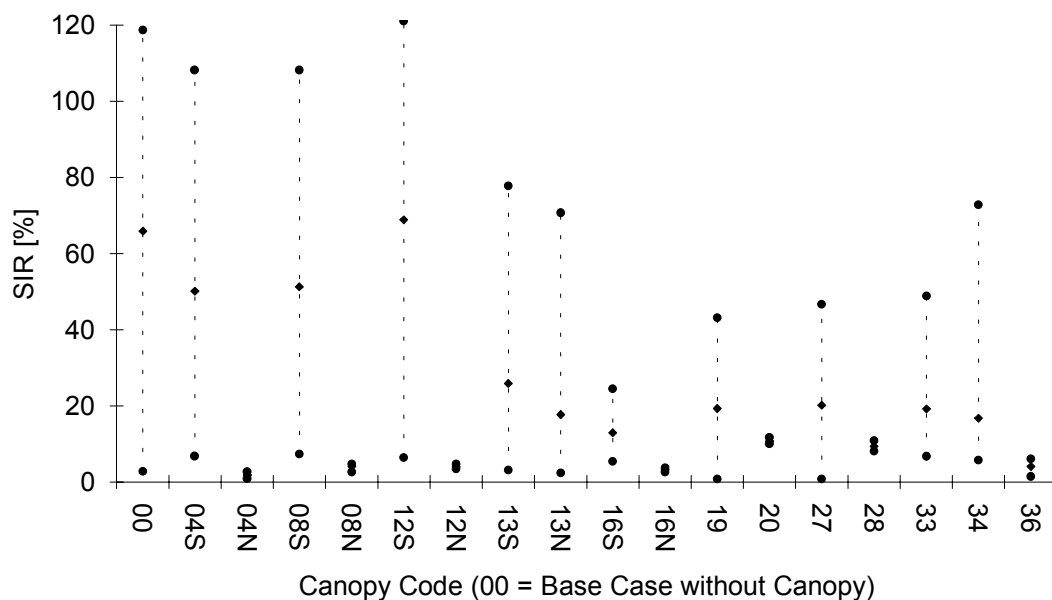


Figure 7.15 Minimum, Maximum, and Average SIR Values at WI = 0.6 with Canopies (Solar Noon, 9/21, Oklahoma City, OK, Sun Alt. = 54.5°)

TABLE 7.12  
 Statistics of SIR Values at WI = 1.2 with 17 Canopy Configurations  
 at Sun Alt. = 54.5° (Solar Noon, 9/21, Oklahoma City, OK)

Canopy Code *	Min [%]	Max [%]	Ave [%]	SD [%]	Canopy Code *	Min [%]	Max [%]	Ave [%]	SD [%]
04S	5.4	109	21.4	38.7	04N	0.7	2.6	1.2	0.7
08S	6.1	108	21.5	38.1	08N	1.7	2.4	2.1	0.3
12S	5.9	80.5	17.3	27.9	12N	1.7	2.4	2.1	0.3
13S	3.9	6.9	5.0	1.0	13N	2.3	94.0	16.6	34.2
16S	4.6	8.0	6.3	1.3	16N	1.5	1.8	1.6	0.1
19	1.5	37.6	7.6	13.3					
20	5.2	5.6	5.4	0.1					
27	1.5	30.2	6.4	10.5					
28	3.9	4.9	4.5	0.3					
33	5.4	26.7	8.7	7.9					
34	3.5	17.8	6.4	5.0					
36	1.0	3.9	2.4	1.2					

\* See Table 4.8 for Canopy Code (S = South, N = North)

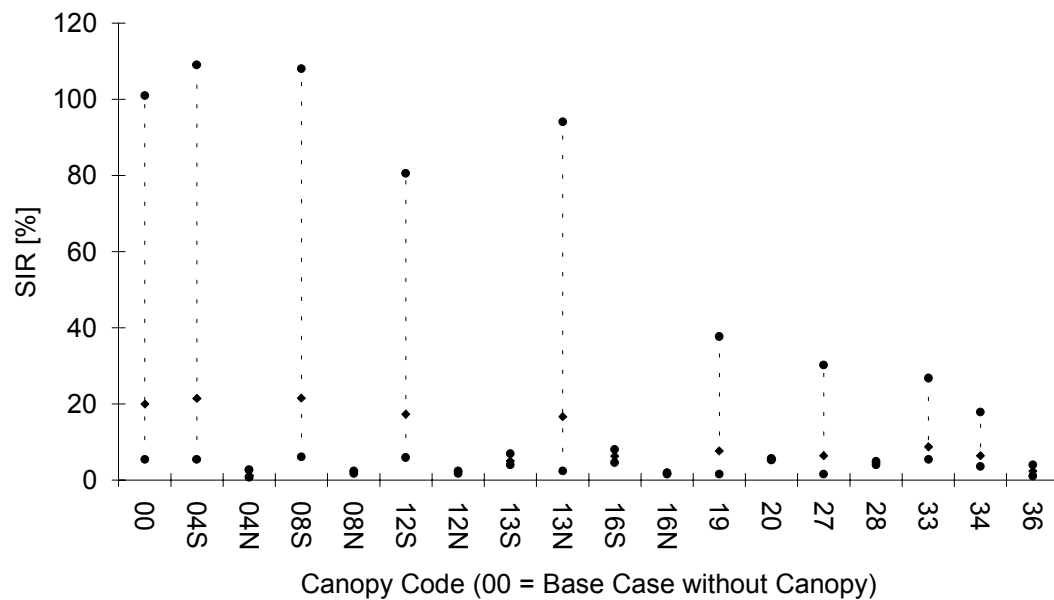


Figure 7.16 Minimum, Maximum, and Average SIR Values at WI = 1.2 with Canopies (Solar Noon, 9/21, Oklahoma City, OK, Sun Alt. = 54.5°)

TABLE 7.13  
 Statistics of SIR Values at WI = 1.8 with 17 Canopy Configurations  
 at Sun Alt. = 54.5° (Solar Noon, 9/21, Oklahoma City, OK)

Canopy Code *	Min [%]	Max [%]	Ave [%]	SD [%]	Canopy Code *	Min [%]	Max [%]	Ave [%]	SD [%]
04S	5.4	10.3	7.5	2.0	04N	0.5	0.9	0.7	0.1
08S	4.9	8.6	6.8	1.5	08N	0.8	1.6	1.2	0.3
12S	4.6	7.0	5.9	0.9	12N	0.7	1.7	1.2	0.4
13S	3.1	6.9	5.1	1.4	13N	2.1	3.2	2.6	0.4
16S	3.9	6.9	5.2	1.3	16N	0.6	0.8	0.7	0.1
19	1.5	6.3	3.7	1.8					
20	2.5	3.2	2.9	0.3					
27	1.5	4.3	2.8	1.0					
28	2.1	3.0	2.5	0.3					
33	3.9	6.1	5.2	0.9					
34	3.3	4.0	3.6	0.3					
36	0.7	1.8	1.1	0.5					

\* See Table 4.8 for Canopy Code (S = South, N = North)

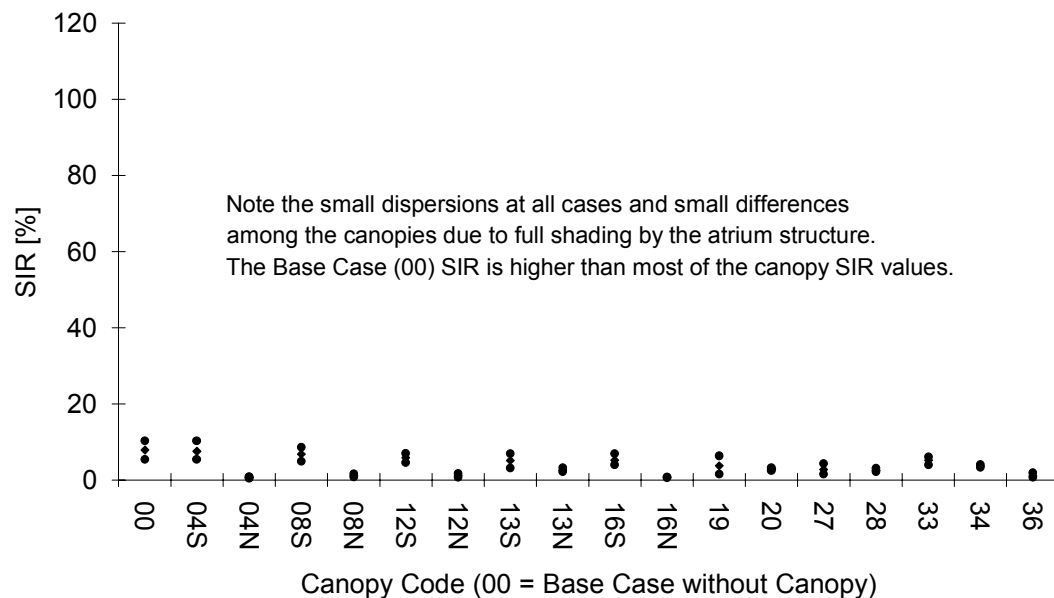


Figure 7.17 Minimum, Maximum, and Average SIR Values at WI = 1.8 with Canopies (Solar Noon, 9/21, Oklahoma City, OK, Sun Alt. = 54.5°)

TABLE 7.14  
 Statistics of SIR Values at WI = 2.4 with 17 Canopy Configurations  
 at Sun Alt. = 54.5° (Solar Noon, 9/21, Oklahoma City, OK)

Canopy Code *	Min [%]	Max [%]	Ave [%]	SD [%]	Canopy Code *	Min [%]	Max [%]	Ave [%]	SD [%]
04S	3.1	5.4	4.2	0.8	04N	0.3	0.7	0.6	0.1
08S	2.6	4.9	3.9	0.8	08N	0.7	0.9	0.7	0.1
12S	1.7	4.4	3.0	1.0	12N	0.3	0.8	0.6	0.2
13S	1.7	3.1	2.5	0.5	13N	0.8	2.7	1.6	0.8
16S	2.0	3.7	2.8	0.5	16N	0.3	0.8	0.6	0.2
19	0.8	1.8	1.3	0.4					
20	1.5	2.1	1.8	0.3					
27	0.8	2.1	1.5	0.5					
28	1.0	1.7	1.5	0.2					
33	1.7	3.9	2.8	0.8					
34	0.9	2.3	1.6	0.4					
36	0.5	1.3	0.9	0.3					

\* See Table 4.8 for Canopy Code (S = South, N = North)

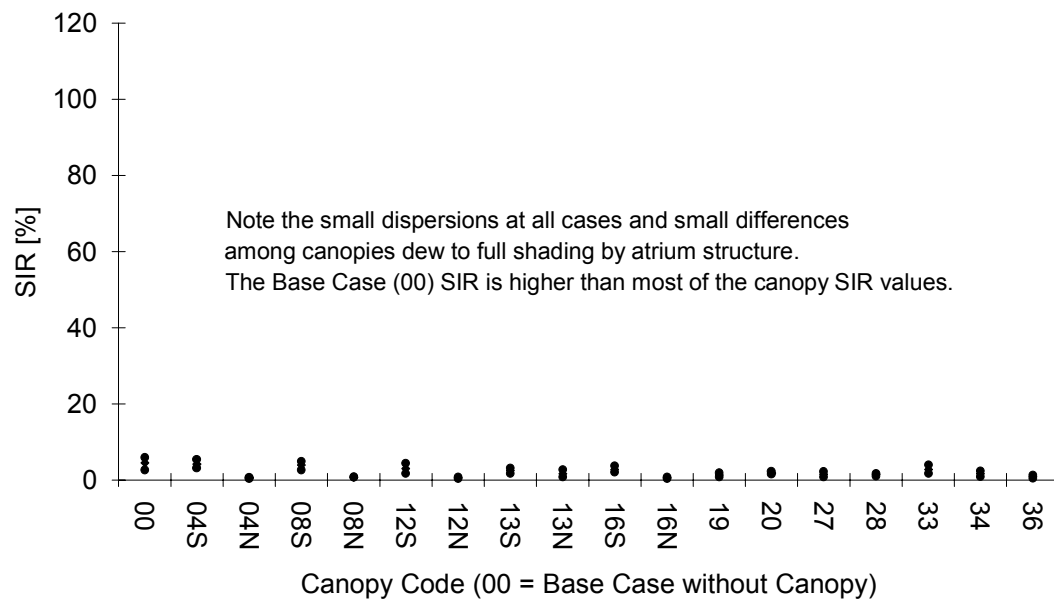
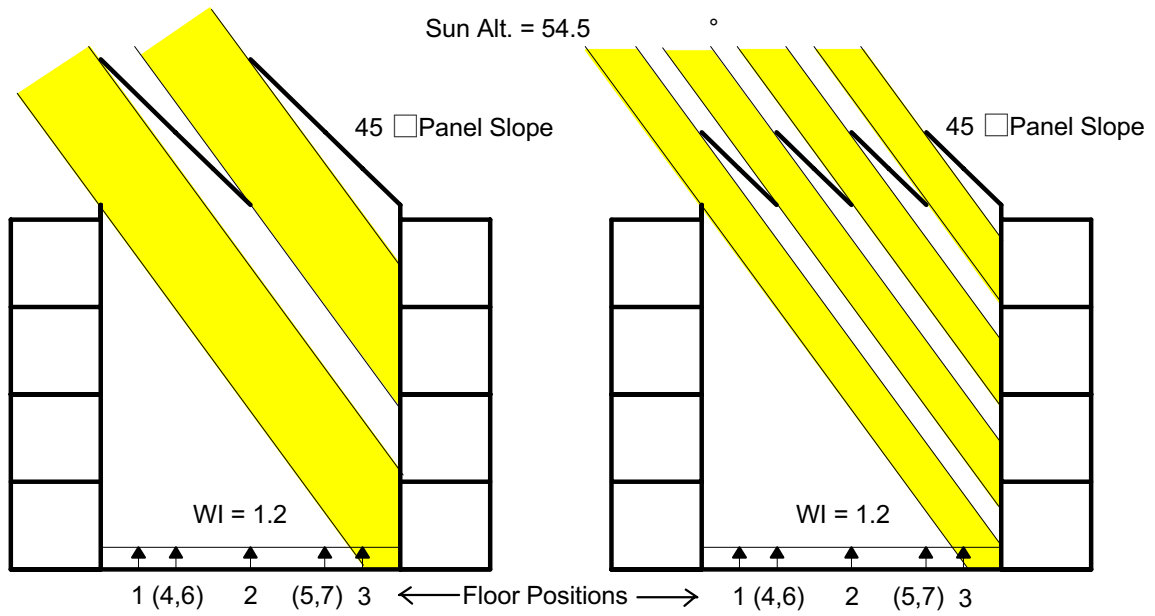


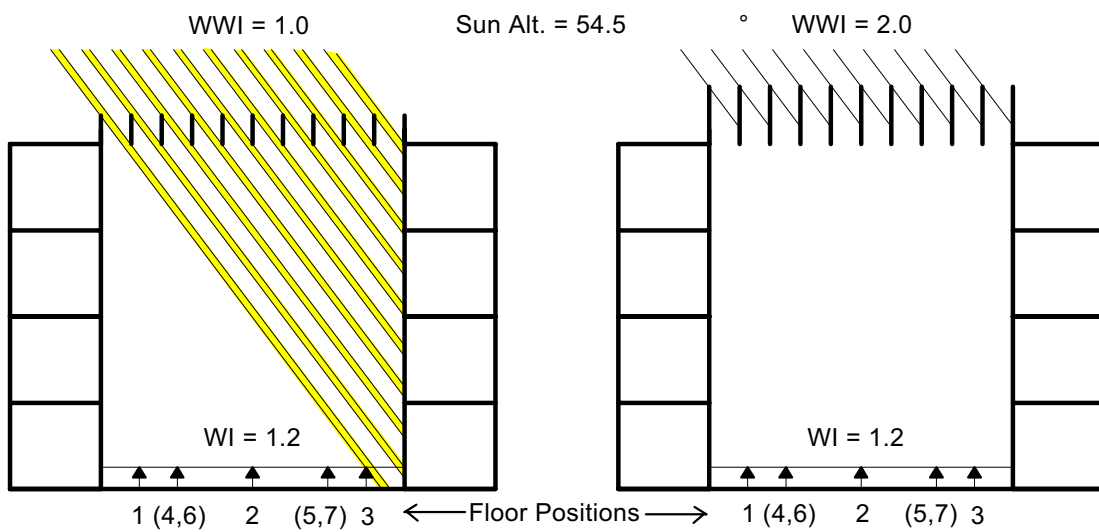
Figure 7.18 Minimum, Maximum, and Average SIR Values at WI = 2.4 with Canopies (Solar Noon, 9/21, Oklahoma City, OK, Sun Alt. = 54.5°)





a. Sawtooth Canopy 04S

b. Sawtooth Canopy 08S



a. Waffle Skylight 34

b. Waffle Skylight 36

Figure 7.19 Sunlight Penetration Diagrams for WI = 1.2 at Sun Alt. = 54.5°  
(Solar Noon, 9/21, Oklahoma City, OK)

Tables 7.15 through 7.18 and Figures 7.20 through 7.23 show the SIR values at solar noon (sun alt. = 22.0°) on December 21 in Minneapolis, MN. As previously shown in Table 5.3, no floor position is exposed to the sun at this sunlight altitude angle. Therefore, all the sunlight illuminances measured were the reflected light from the atrium wall surfaces.

A notable feature at this low sun angle was that several canopy configurations showed higher SIR values than the Base Case SIR (BCSIR) values measured without canopy. Especially, the sawtooth canopies with south-facing apertures (No. 04S, 08S, and 12S) always showed higher SIR values than each BCSIR at each WI value. An extreme case was observed with canopy 04, which resulted in 18.8 % higher SIR value than BCSIR. This is another notable characteristic lighting performance of sawtooth type canopies with south-facing apertures. At a high sun altitude angle, the solid panels block direct beam sunlight. However, at a low sun altitude angle, the bottom surfaces of the solid panels catch the incoming sunlight and reflect it toward the atrium space. Therefore, the spatial distribution and intensity of the reflected light (i.e., luminance) are mainly dependent upon the specularity and reflectance of the bottom surfaces of solid panels. In addition to the photometric properties of the panel surfaces, the geometric relationship between the floor positions and the interior panel surface areas play another critical roll in determining the illuminance levels at floor positions. This can be clearly explained by observing the reduced SIR values as the WI values increased.

Another notable feature was the higher SIR values for the skylights with translucent glazing than those with tinted transparent glazing. With the pyramid skylights, the average "percent difference" between the SIR values of tinted transparent glazing and those of white translucent glazing was about 50 %. This is an interesting character of translucent glazing material. At high sun altitude angles, the translucent glazing resulted in even lower SIR values (for direct sun) than the Hemispherical Transmittance (HT) values (for diffuse skies). However, at low sun altitude angles, it acts similarly to sawtooth canopies. It also catches low-altitude incoming sunlight and diffusely transmits it toward the atrium space. This effect was visually demonstrated in the previous Figures 5.22 and 5.23 which showed the pyramid skylights with transparent and translucent glazing materials, respectively. Even though the video images were captured at the sun altitude angle of 31.3° (solar noon, 12/21, Oklahoma City), the sun angle was low enough to demonstrate the special lighting performance of translucent glazing material.

Most of all, at low sun altitude angles, the impact of atrium well configuration is the most profound in determining the sunlight illuminance levels at floor positions.

TABLE 7.15  
 Statistics of SIR Values at WI = 0.6 with 17 Canopy Configurations  
 at Sun Alt. = 22.0° (Solar Noon, 12/21, Minneapolis, MN)

Canopy Code *	Min [%]	Max [%]	Ave [%]	SD [%]	Canopy Code *	Min [%]	Max [%]	Ave [%]	SD [%]
04S	28.6	39.1	35.2	3.7	04N	0.6	1.4	1.0	0.4
08S	24.3	31.0	27.8	2.7	08N	1.5	3.0	2.1	0.6
12S	18.4	22.8	20.7	1.8	12N	1.5	2.4	1.8	0.3
13S	7.2	23.9	14.8	7.7	13N	1.4	3.8	2.5	0.9
16S	17.1	31.3	23.8	6.7	16N	1.3	1.7	1.5	0.2
19	1.4	6.5	3.5	2.5					
20	6.0	9.6	8.3	1.2					
27	2.9	11.7	6.6	4.1					
28	7.3	11.1	9.6	1.3					
33	1.6	4.4	2.9	1.2					
34	0.6	3.0	1.7	0.8					
36	0.5	0.6	0.5	0.1					

\* See Table 4.8 for Canopy Code (S = South, N = North)

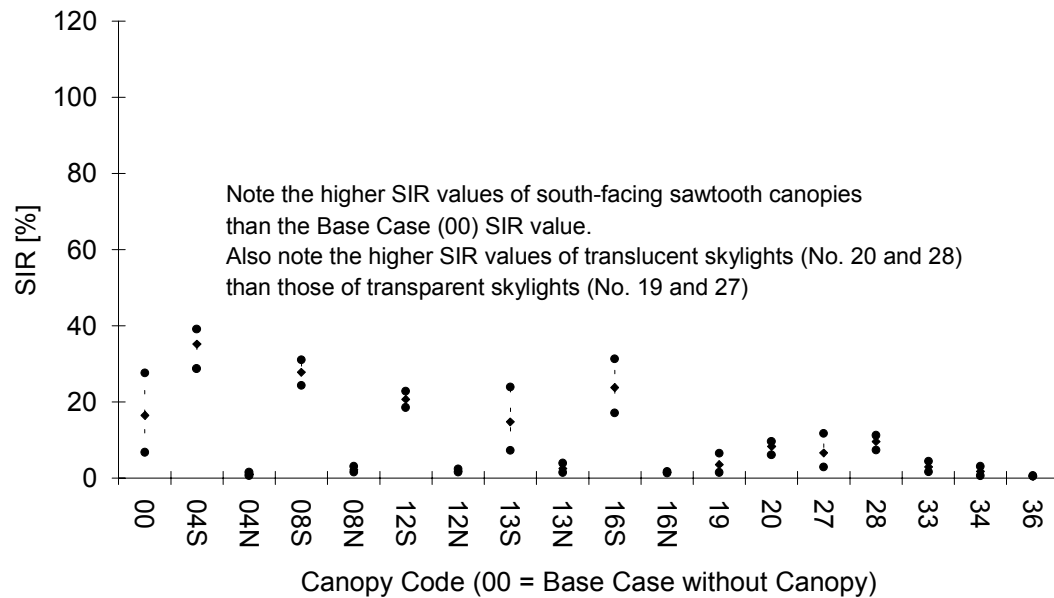


Figure 7.20 Minimum, Maximum, and Average SIR Values at WI = 0.6 with Canopies (Solar Noon, 12/21, Minneapolis, MN, Sun Alt. = 22.0°)

TABLE 7.16  
 Statistics of SIR Values at WI = 1.2 with 17 Canopy Configurations  
 at Sun Alt. = 22.0° (Solar Noon, 12/21, Minneapolis, MN)

Canopy Code *	Min [%]	Max [%]	Ave [%]	SD [%]	Canopy Code *	Min [%]	Max [%]	Ave [%]	SD [%]
04S	13.0	17.9	15.7	1.5	04N	1.0	3.2	1.6	0.8
08S	9.7	14.9	12.7	2.1	08N	0.5	2.8	1.1	0.8
12S	7.8	13.1	10.6	1.7	12N	1.0	3.6	1.7	0.9
13S	1.3	6.0	4.3	1.9	13N	0.6	2.8	1.4	0.7
16S	5.1	10.3	8.6	1.9	16N	0.5	4.6	1.4	1.5
19	0.5	1.9	1.3	0.5					
20	2.4	5.0	3.8	1.1					
27	1.4	2.2	1.8	0.3					
28	2.8	5.0	4.1	0.8					
33	0.6	1.5	1.1	0.4					
34	0.5	2.3	1.1	0.7					
36	0.5	2.8	1.1	0.9					

\* See Table 4.8 for Canopy Code (S = South, N = North)

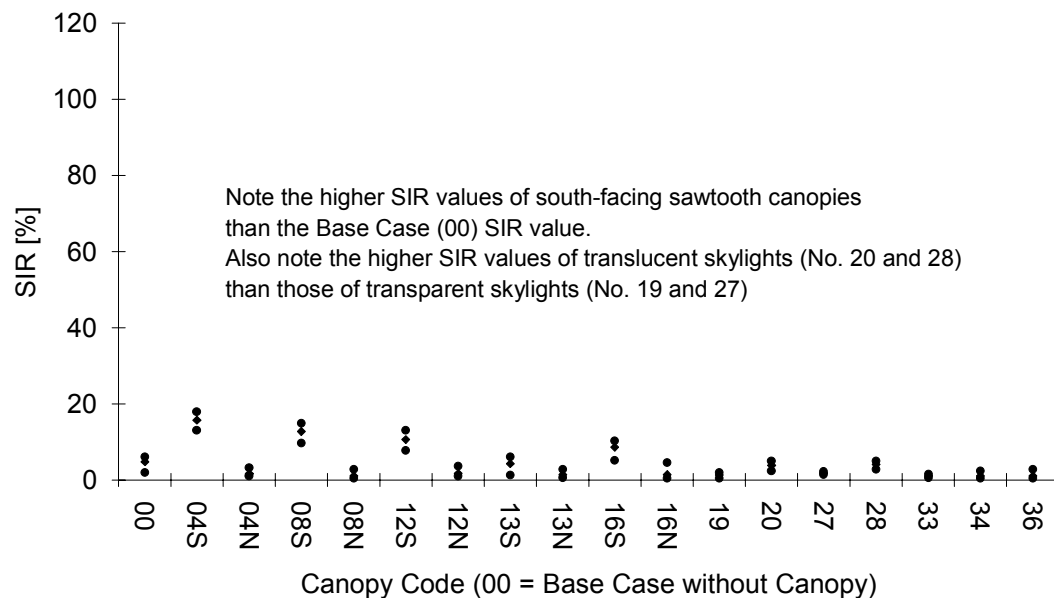


Figure 7.21 Minimum, Maximum, and Average SIR Values at WI = 1.2 with Canopies (Solar Noon, 12/21, Minneapolis, MN, Sun Alt. = 22.0°)

TABLE 7.17  
 Statistics of SIR Values at WI = 1.8 with 17 Canopy Configurations  
 at Sun Alt. = 22.0° (Solar Noon, 12/21, Minneapolis, MN)

Canopy Code *	Min [%]	Max [%]	Ave [%]	SD [%]	Canopy Code *	Min [%]	Max [%]	Ave [%]	SD [%]
04S	3.1	22.1	7.4	6.6	04N	0.3	0.4	0.3	0.0
08S	3.5	5.4	4.4	0.9	08N	0.6	0.8	0.7	0.1
12S	2.8	15.4	4.9	4.6	12N	0.3	0.7	0.5	0.2
13S	2.5	8.2	4.4	2.0	13N	2.1	11.1	3.7	3.3
16S	2.8	5.3	3.8	1.1	16N	0.3	0.7	0.5	0.2
19	1.5	7.2	3.0	2.0					
20	1.2	2.1	1.7	0.3					
27	1.6	8.9	3.3	2.6					
28	1.4	2.1	1.7	0.2					
33	3.1	16.8	5.7	4.9					
34	2.5	13.0	4.7	3.7					
36	1.4	2.1	1.7	0.2					

\* See Table 4.8 for Canopy Code (S = South, N = North)

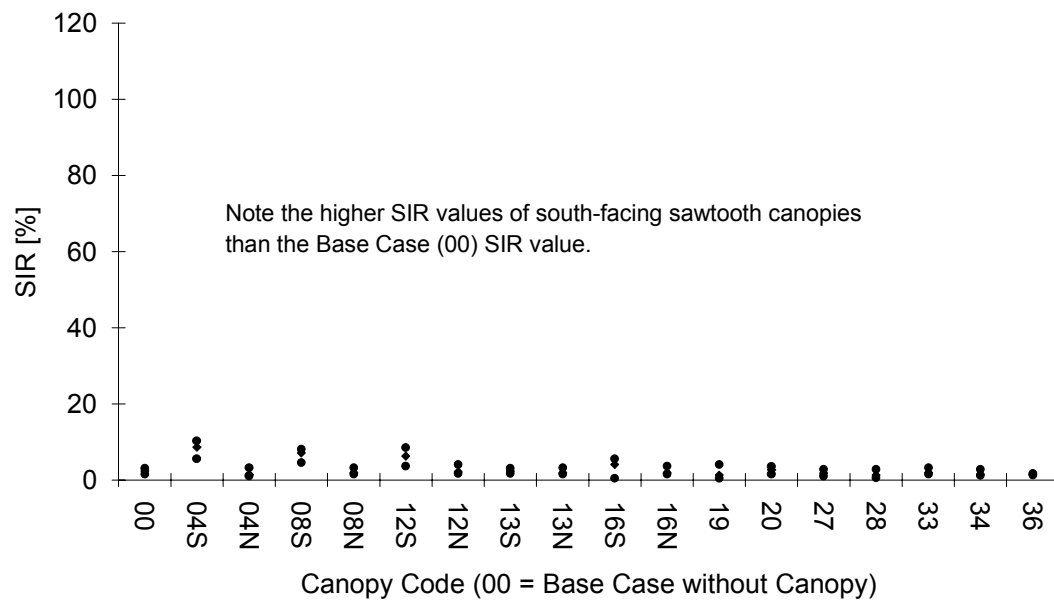


Figure 7.22 Minimum, Maximum, and Average SIR Values at WI = 1.8 with Canopies (Solar Noon, 12/21, Minneapolis, MN, Sun Alt. = 22.0°)

TABLE 7.18  
 Statistics of SIR Values at WI = 2.4 with 17 Canopy Configurations  
 at Sun Alt. = 22.0° (Solar Noon, 12/21, Minneapolis, MN)

Canopy Code *	Min [%]	Max [%]	Ave [%]	SD [%]	Canopy Code *	Min [%]	Max [%]	Ave [%]	SD [%]
04S	2.3	6.0	4.8	1.4	04N	Sawtooth canopies oriented to north were excluded due to too low illuminances			
08S	1.8	5.0	3.8	1.4	08N				
12S	1.8	5.0	3.5	1.2	12N				
13S	0.5	1.7	1.2	0.4	13N				
16S	0.5	3.0	1.9	1.0	16N				
19	0.3	1.2	0.6	0.3					
20	1.2	1.9	1.6	0.2					
27	0.5	1.5	0.8	0.4					
28	0.5	1.9	1.4	0.4					
33	0.7	3.6	1.5	1.3					
34	0.5	2.8	1.2	1.0					
36	0.5	2.3	1.0	0.8					

\* See Table 4.8 for Canopy Code (S = South, N = North)

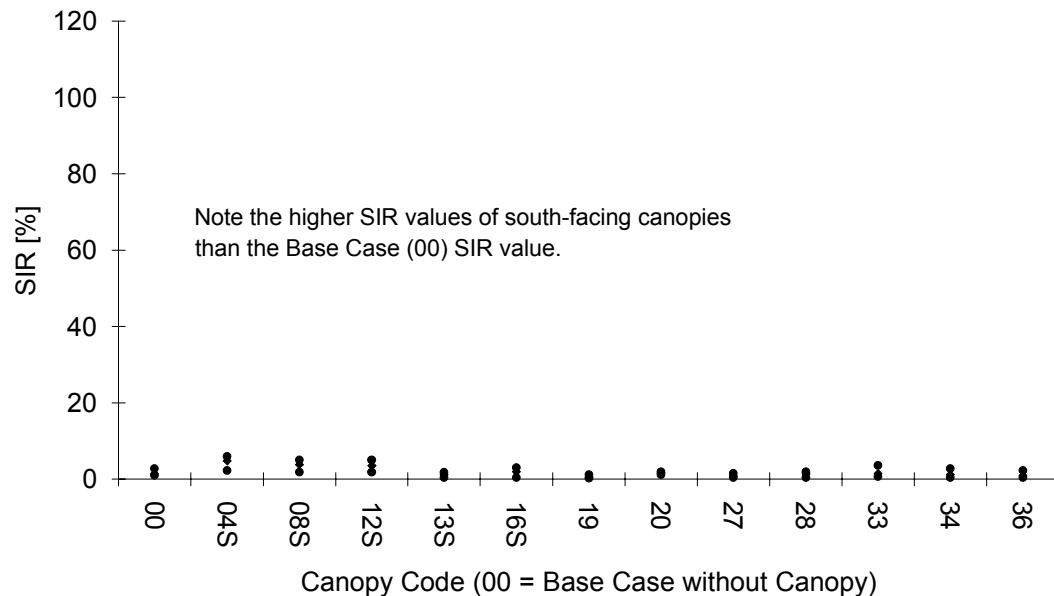


Figure 7.23 Minimum, Maximum, and Average SIR Values at WI = 2.4 with Canopies (Solar Noon, 12/21, Minneapolis, MN, Sun Alt. = 22.0°)

Figures 7.24 through 7.31 show the average SIR values with canopies at the nine different rounded-off sun altitude angles for each WI value. As revealed in Figures 7.24, 7.26, 7.28, and 7.30, the sawtooth canopies with south-facing apertures (No. 04S, 08S, 12S, 13S, and 16S) and those with north-facing sloping apertures (No. 13N, 16N) showed different SIR values at different sun altitude angles.

Figures 7.25, 7.27, 7.29, and 7.31 also demonstrate that skylights with transparent glazing and waffle skylights resulted in different SIR values at different sun altitude angles. Meanwhile, the sawtooth canopies with north-facing vertical apertures (No. 04N, 08N, and 12N) and skylights with translucent glazing (No. 20 and 28) showed almost constant SIR values at a given WI value, even though the sun altitude angle varied from 84° to 22°.

The most dramatic changes in the average SIR values with the varying sun altitude angles were observed with waffle skylights (No., 33, 34, and 36). In addition, when the average SIR values of the waffle skylights at each sun altitude angle were compared at different WI values, it was also known that WI values also affected the SIR values. From these two observations, it can be said that the waffle skylight systems are the most geometry sensitive canopy systems. This is due to the geometric nature of the waffle skylights. The large horizontal opening area and the opaque waffle walls play totally different rolls at different sun altitude angles and different WI values. At high sun altitude angles, the opaque waffle walls do not block the beam sunlight, but the transmission characteristics of the horizontal apertures mainly determine the intensity and spatial distributions of transmitted sunlight. On the contrary, at medium to low sun altitude angles, the waffle walls substantially block the beam sunlight and play a major role in determining the interior illuminance levels and spatial distribution.

The above statements were well confirmed when the average SIR values of skylights with tinted transparent glazing (No. 19 and 27) were observed. Since the two skylights did not have large opaque areas, the variations with the sun altitude angles were not as profound as those of waffle skylights.

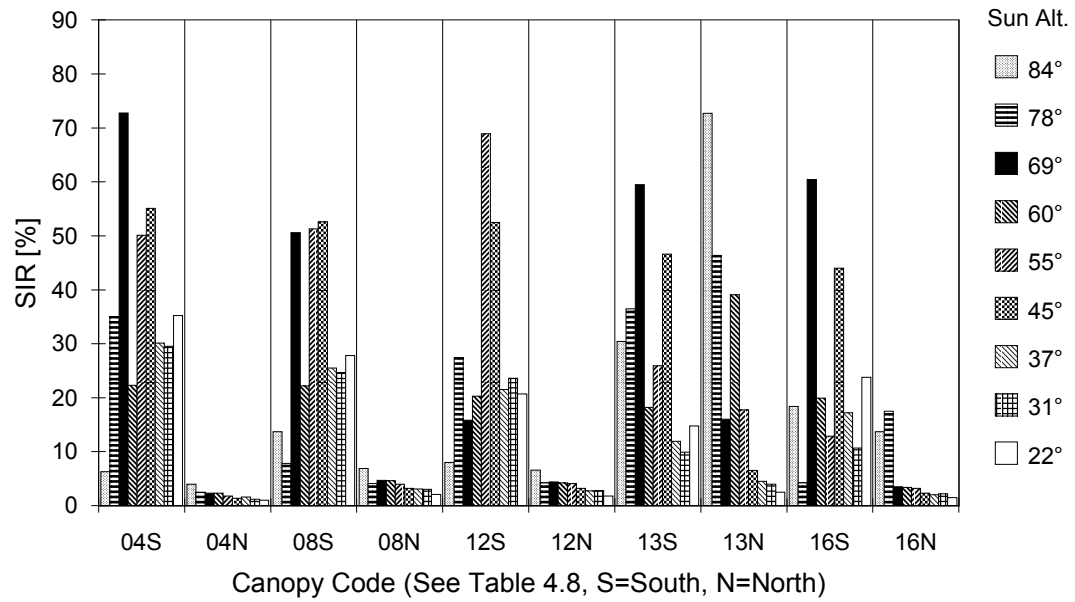


Figure 7.24 Sunlight Illuminance Ratios at WI = 0.6 (Atrium A2) with Sawtooth Canopies at Different Sun Altitude Angles

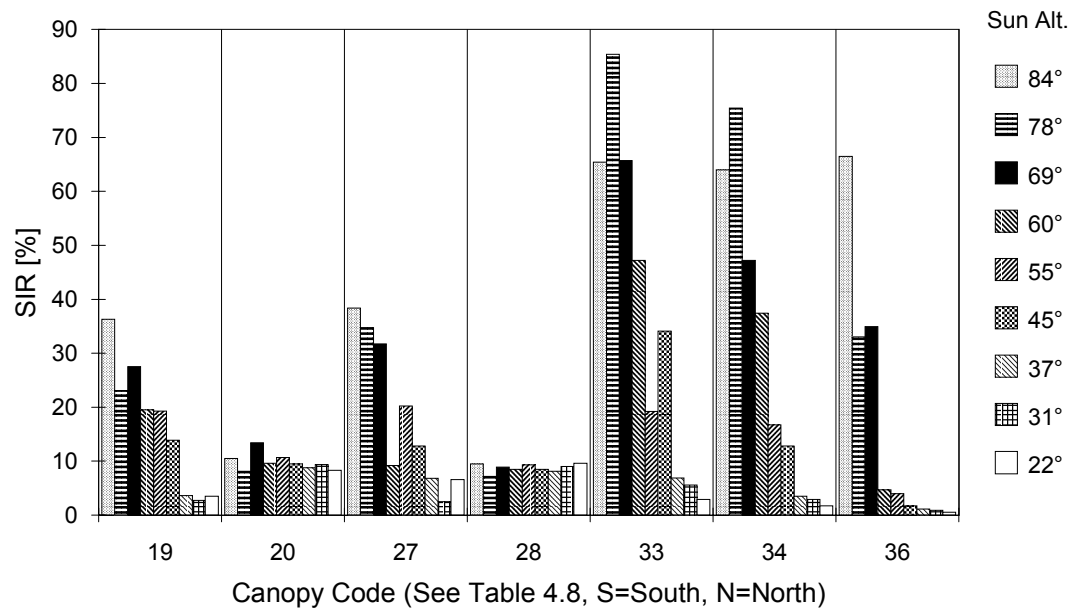


Figure 7.25 Sunlight Illuminance Ratios at WI = 0.6 (Atrium A2) with Skylight Canopies at Different Sun Altitude Angles



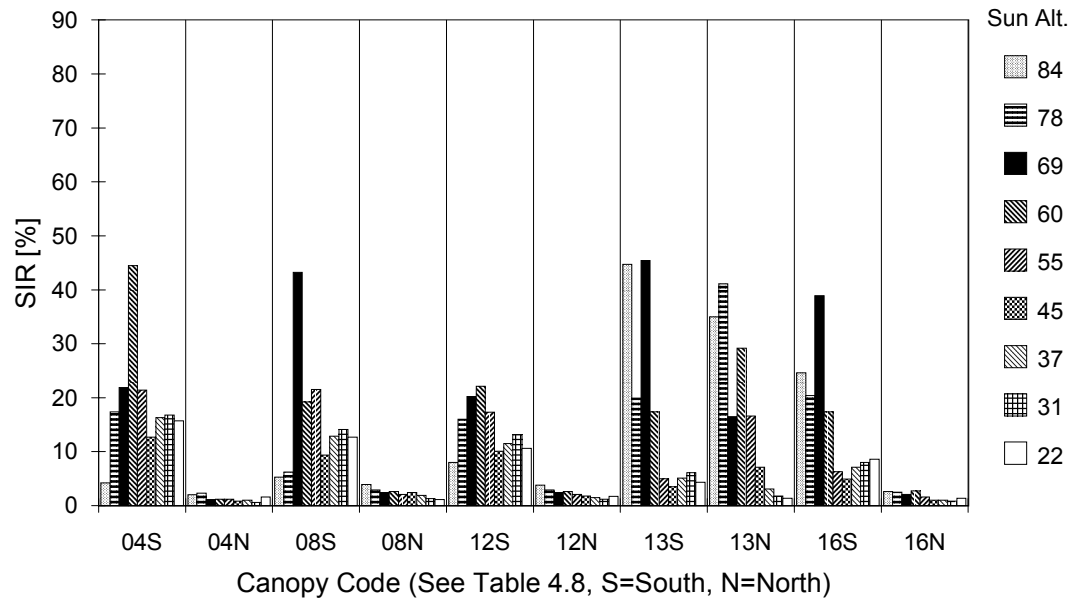


Figure 7.26 Sunlight Illuminance Ratios at WI = 1.2 (Atrium A4) with Sawtooth Canopies at Different Sun Altitude Angles

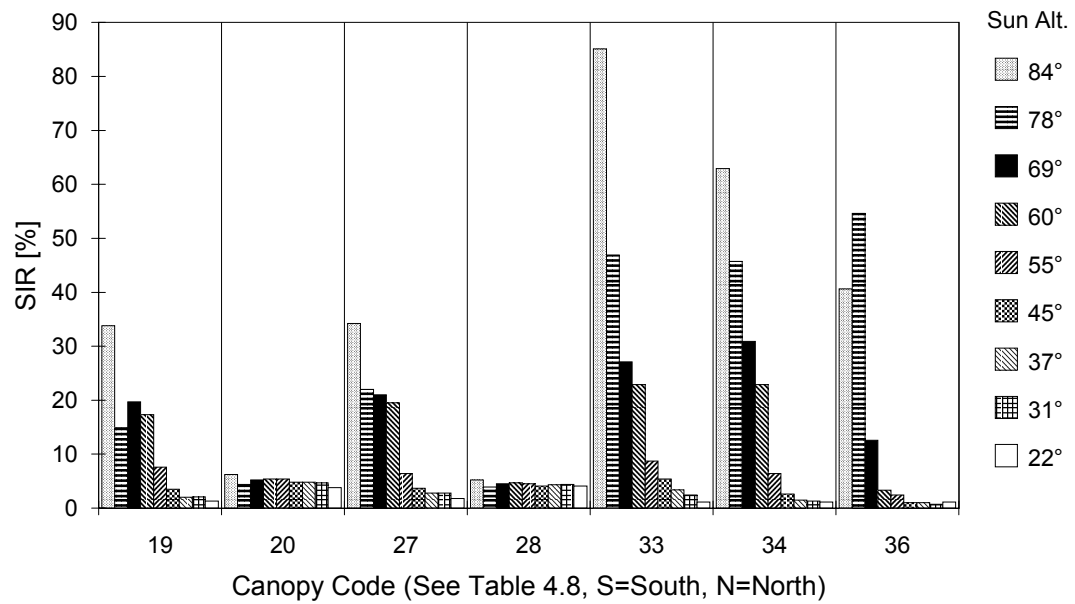


Figure 7.27 Sunlight Illuminance Ratios at WI = 1.2 (Atrium A4) with Skylight Canopies at Different Sun Altitude Angles

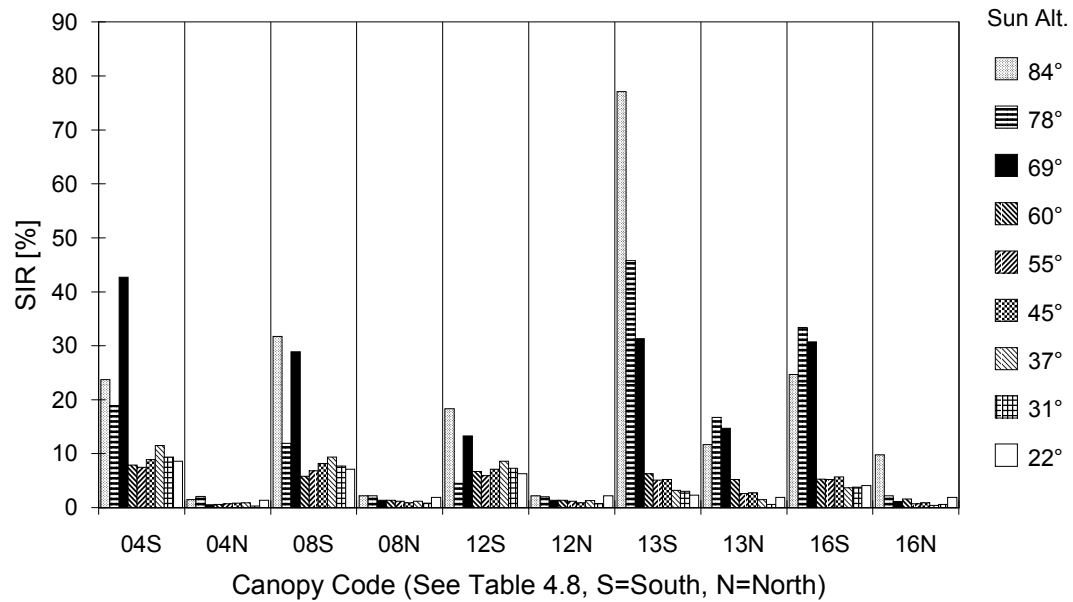


Figure 7.28 Sunlight Illuminance Ratios at WI = 1.8 (Atrium A6) with Sawtooth Canopies at Different Sun Altitude Angles

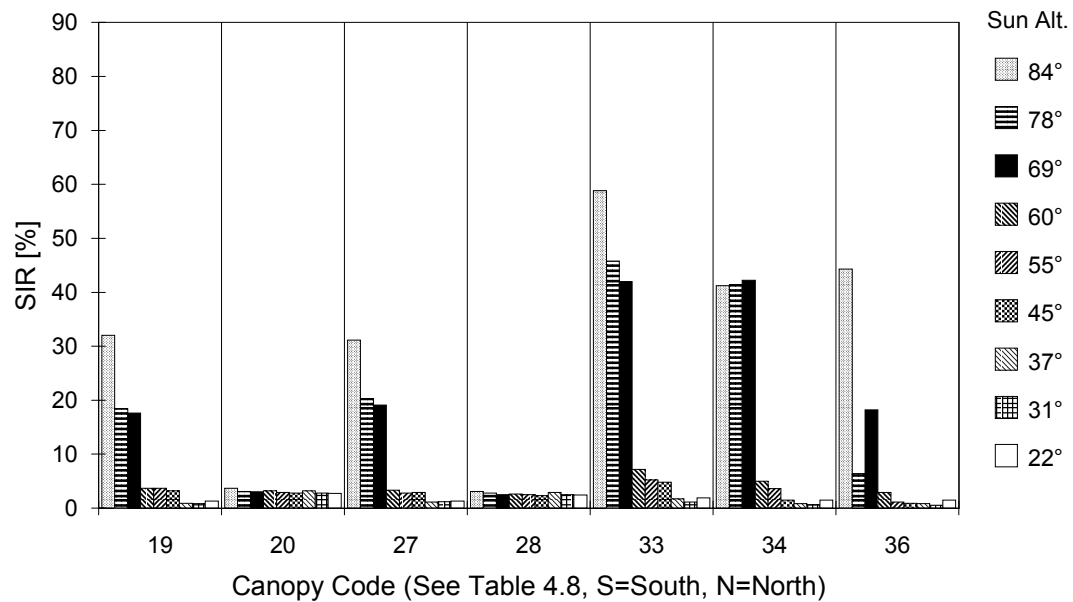


Figure 7.29 Sunlight Illuminance Ratios at WI = 1.8 (Atrium A6) with Skylight Canopies at Different Sun Altitude Angles

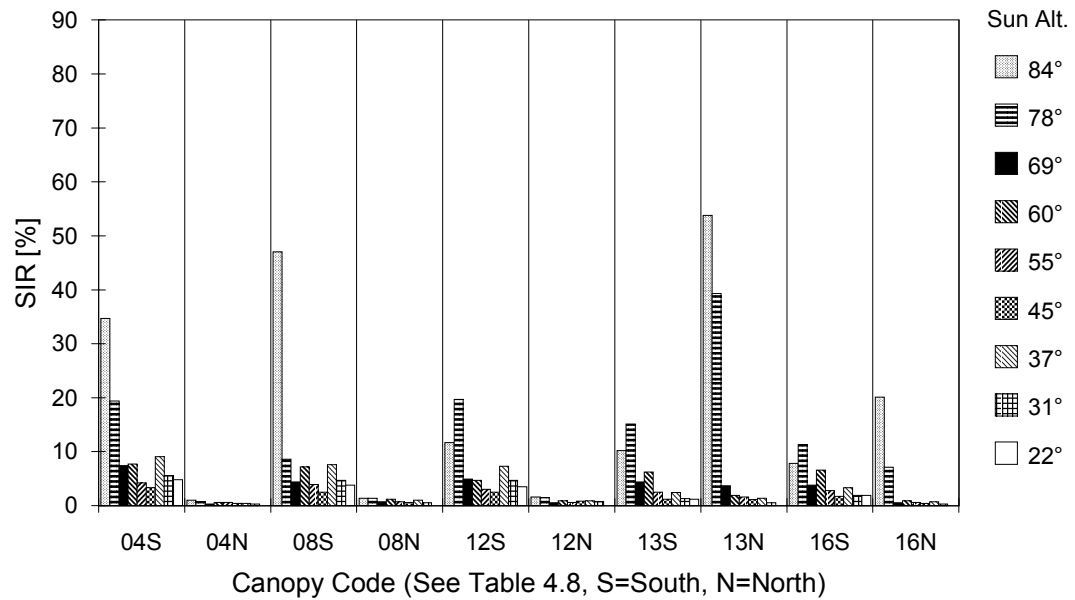


Figure 7.30 Sunlight Illuminance Ratios at WI = 2.4 (Atrium A8) with Sawtooth Canopies at Different Sun Altitude Angles

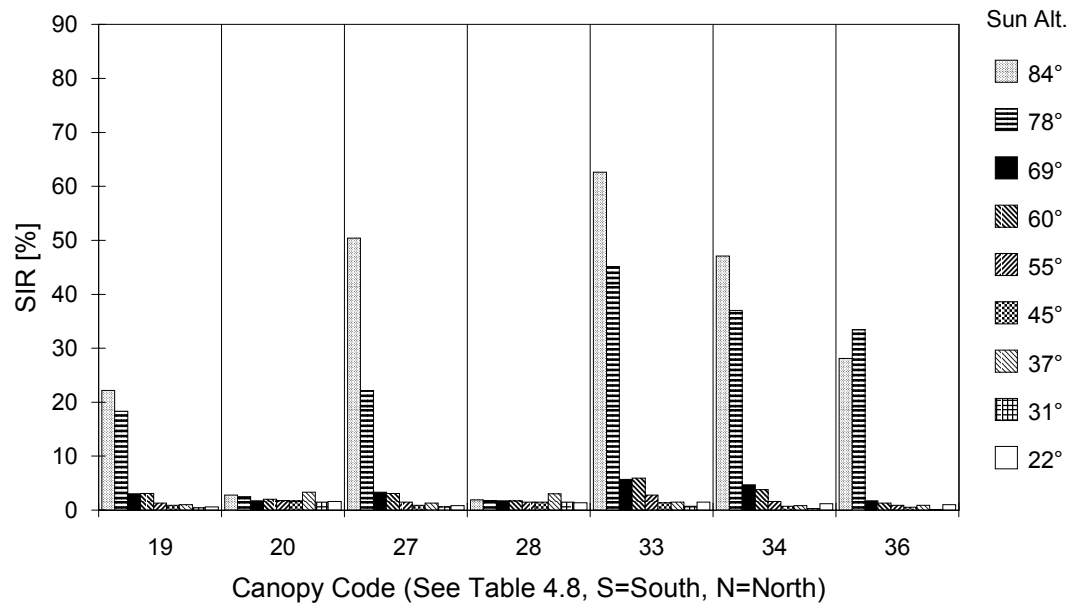


Figure 7.31 Sunlight Illuminance Ratios at WI = 2.4 (Atrium A8) with Skylight Canopies at Different Sun Altitude Angles

## 7.2 SUNLIGHT LUMINANCE DISTRIBUTIONS IN ATRIA

### 7.2.1 Sunlight Luminance Distributions without Canopy

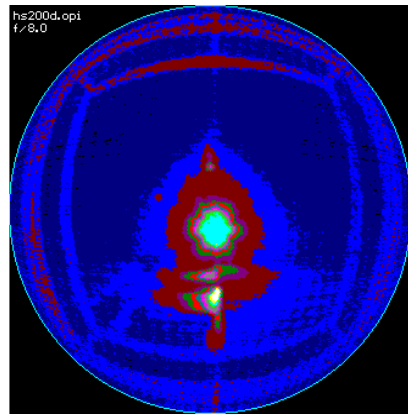
The video-based luminance mapping system was again used to map luminance distribution patterns in the sunlit atria. The atria with WI values of 0.6 (atrium A2), 1.2 (atrium A4), 1.8 (atrium A6), and 2.4 (atrium A8) were included in this test. The sun altitude angles used were  $84.0^\circ$  and  $31.3^\circ$  which represented the noon sun altitudes on June 21 in Houston and December 21 in Oklahoma City, respectively.

At the high sun altitude angle, the fisheye lens of the luminance mapping system was inserted into the bottom of the model stand the same as in the daylight luminance distribution mapping. On the contrary, at the low sun angle, the whole video camera assembly was placed in the atrium space and moved up and down to match the different WI values.

The video images in Figure 7.32 show the sunlight luminance distribution maps at sun altitude angle of  $84.0^\circ$  for the four WI values. As shown in the images, the luminances on the north wall were somewhat higher than the other walls, because the sun was still biased to the south direction.

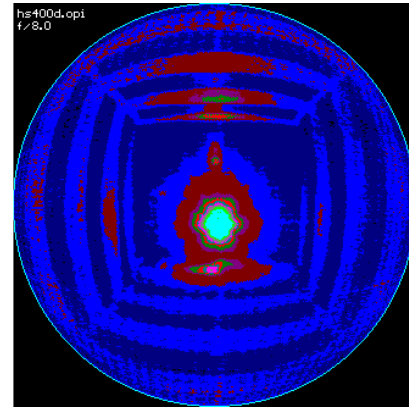
Figures 33 through 36 show the sunlight LI values. The four figures indicate that the luminance distribution patterns on the south and the west walls were almost consistent throughout the varying WI values. On the contrary, the luminances high on of the north wall increased as the WI increased. Figures 7.37 through 7.40 show the average LI values on the three walls for each WI value. Tables 7.19 through 7.22 summarize the Luminance Ratios (LR) between two contiguous wall areas which were previously specified in Figure 6.52. In general, at this high sun altitude, the LR values were almost the same as those for daylight. It can also be said that the atrium well effects on the wall luminance distributions were very minimal. In addition, the illuminance level at the floor positions were mainly due to the direct beam sunlight.

With these video images, it can be easily imagined that the south-facing sawtooth canopies with vertical apertures effectively kept the direct sunlight from intruding into the atrium spaces at high sun altitude angles.



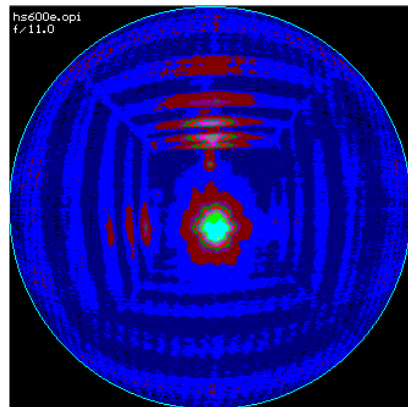
South

a. WI = 0.6 (Atrium A2, f/8)



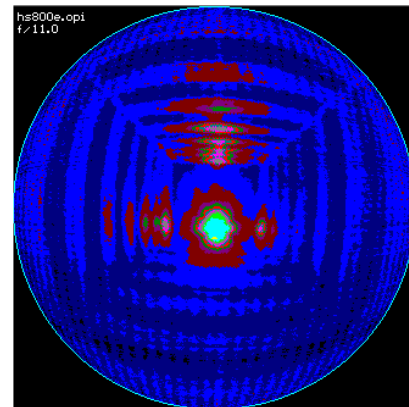
South

b. WI = 1.2 (Atrium A4, f/8)



South

c. WI = 1.8 (Atrium A6, f/11)



South

d. WI = 2.4 (Atrium A8, f/11)

Figure 7.32 Video Images of Sunlight Luminance Distributions without Canopy at Sun Alt. =  $84.0^\circ$  (Solar Noon, 6/21, Houston, TX)

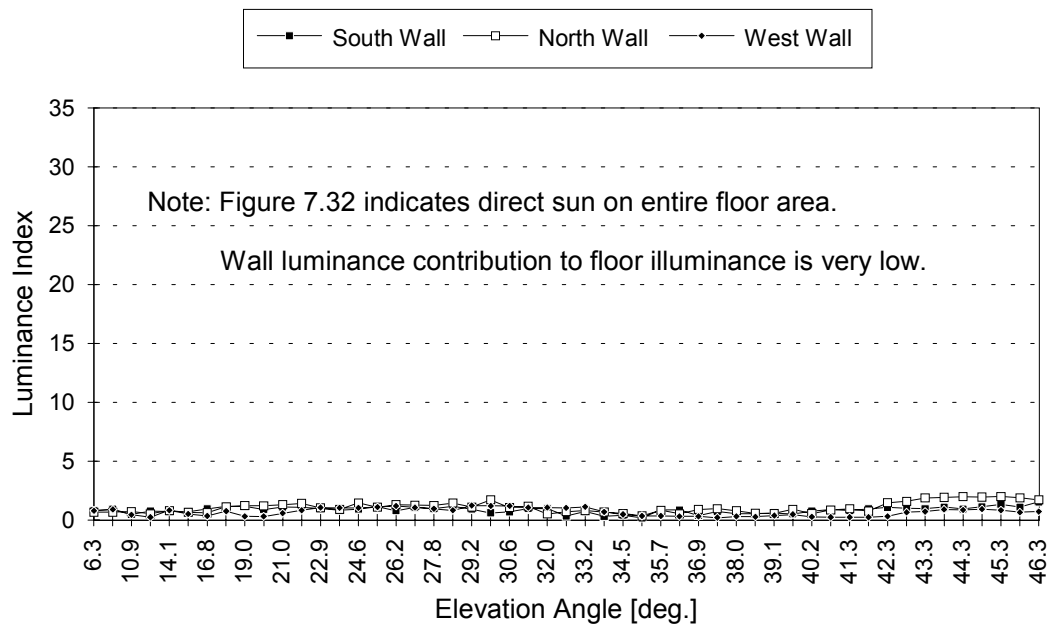


Figure 7.33 Sunlight Luminance Index Values for WI = 0.6 without Canopy at Sun Alt. = 84.0° (Solar Noon, 6/21, Houston, TX)

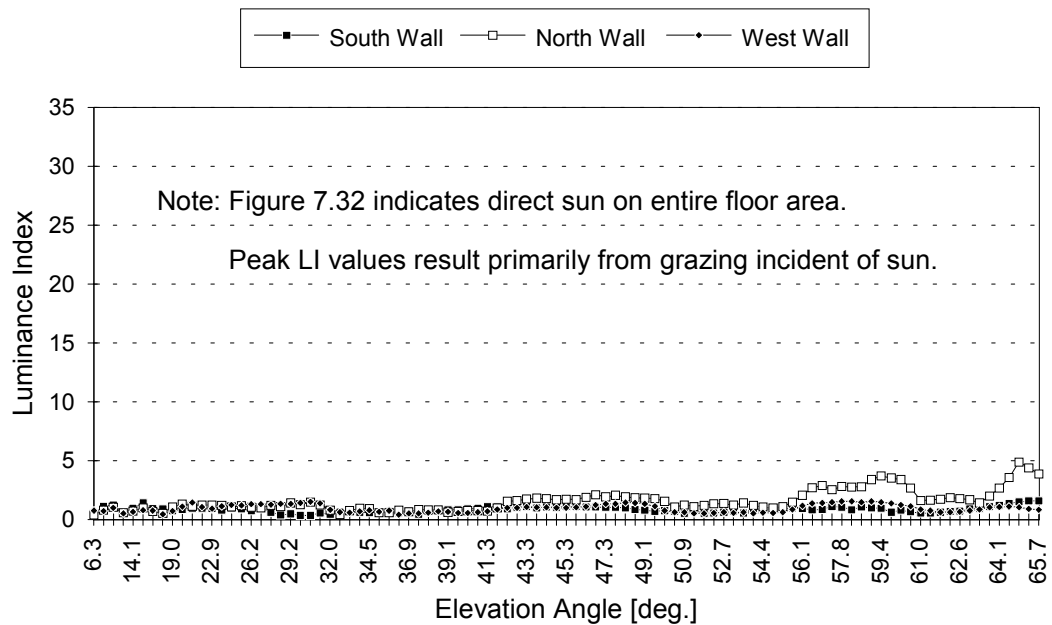


Figure 7.34 Sunlight Luminance Index Values for WI = 1.2 without Canopy at Sun Alt. = 84.0° (Solar Noon, 6/21, Houston, TX)

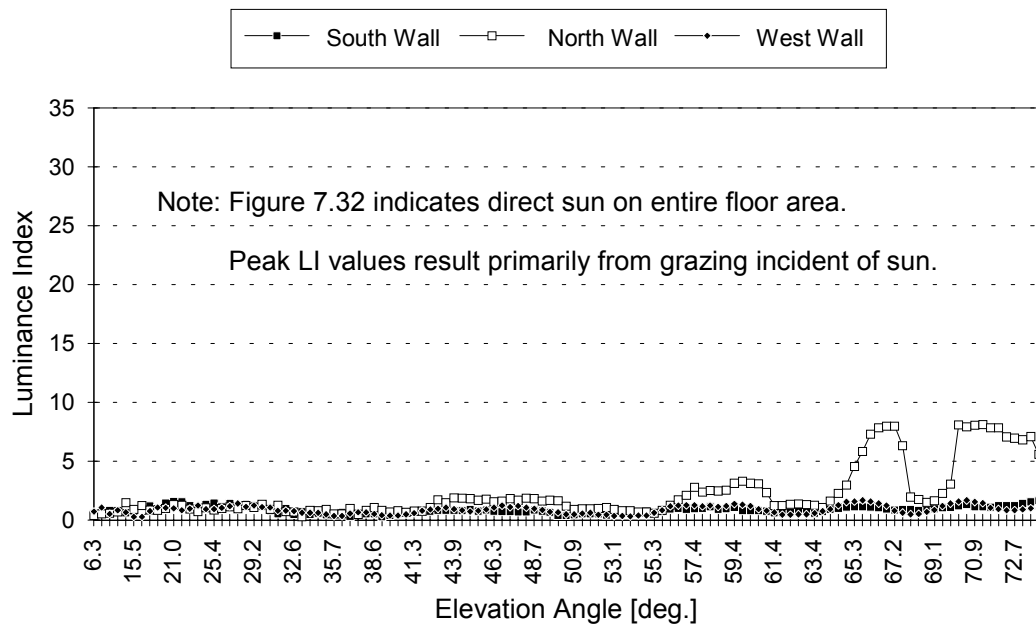


Figure 7.35 Sunlight Luminance Index Values for WI = 1.8 without Canopy at Sun Alt. = 84.0° (Solar Noon, 6/21, Houston, TX)

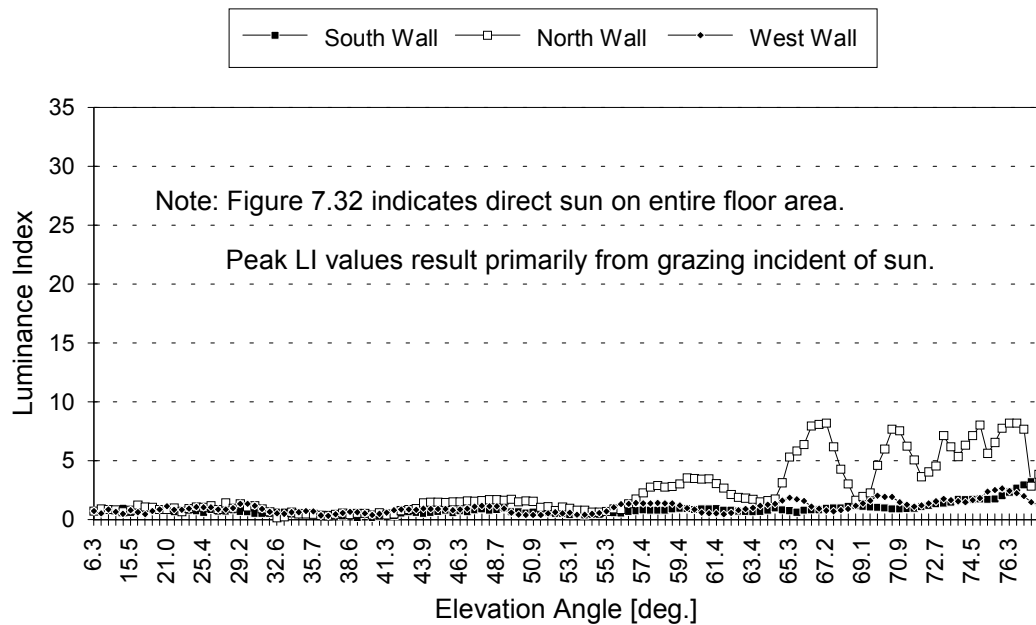


Figure 7.36 Sunlight Luminance Index Values for WI = 2.4 without Canopy at Sun Alt. = 84.0° (Solar Noon, 6/21, Houston, TX)

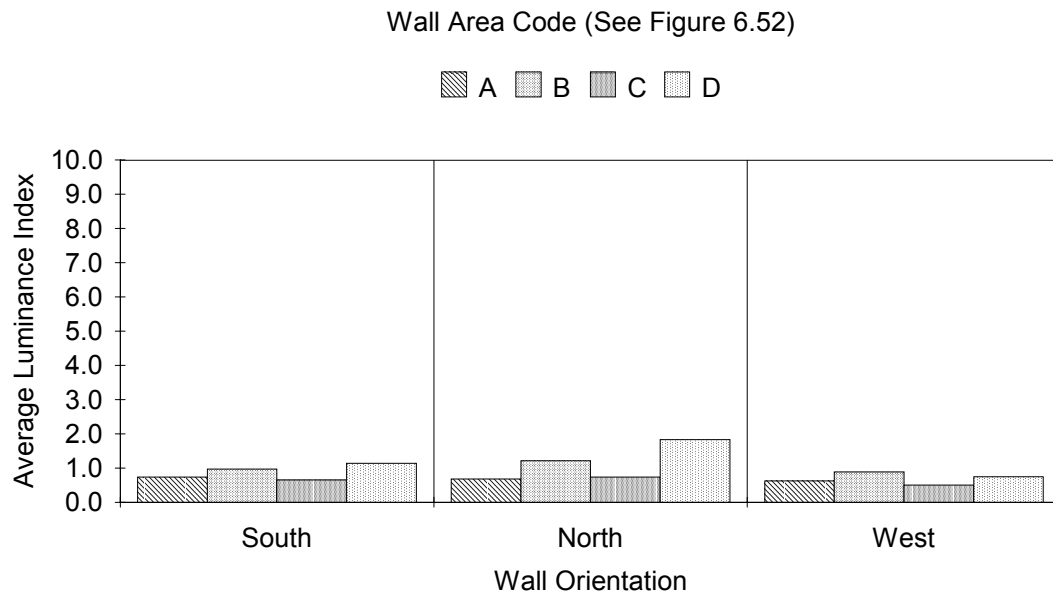


Figure 7.37 Average Sunlight Luminance Index Values for WI = 0.6 at Sun Alt. = 84.0° (Solar Noon, 6/21, Houston, TX)

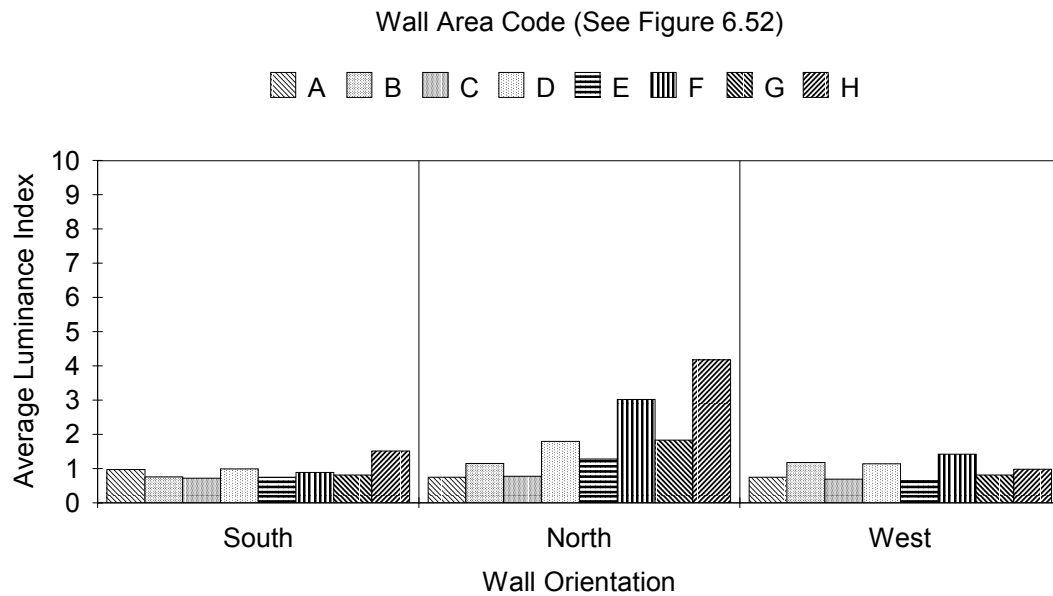


Figure 7.38 Average Sunlight Luminance Index Values for WI = 1.2 at Sun Alt. = 84.0° (Solar Noon, 6/21, Houston, TX)



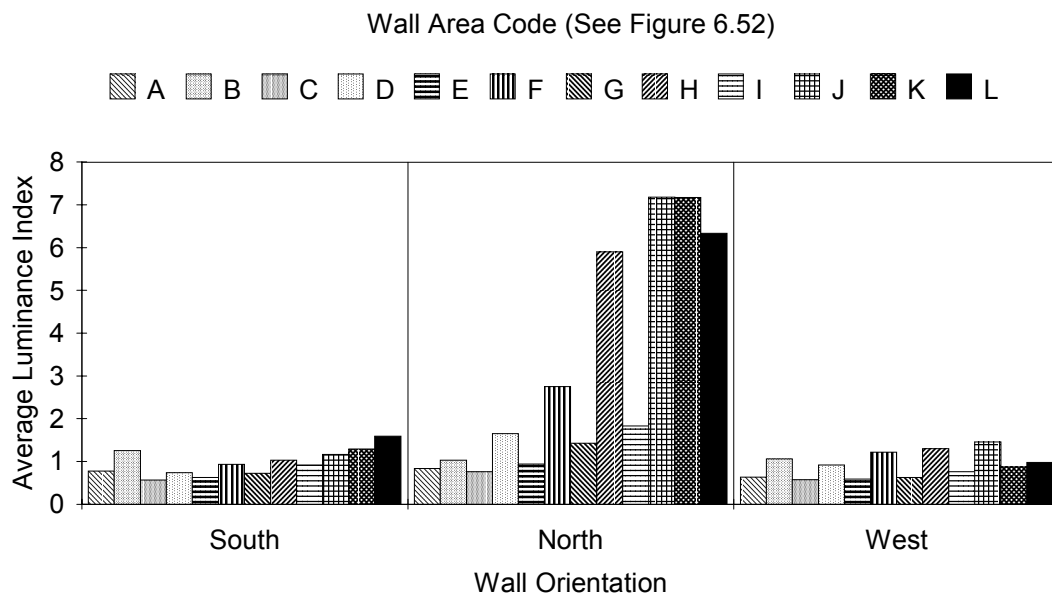


Figure 7.39 Average Sunlight Luminance Index Values for WI = 1.8 at Sun Alt. = 84.0° (Solar Noon, 6/21, Houston, TX)

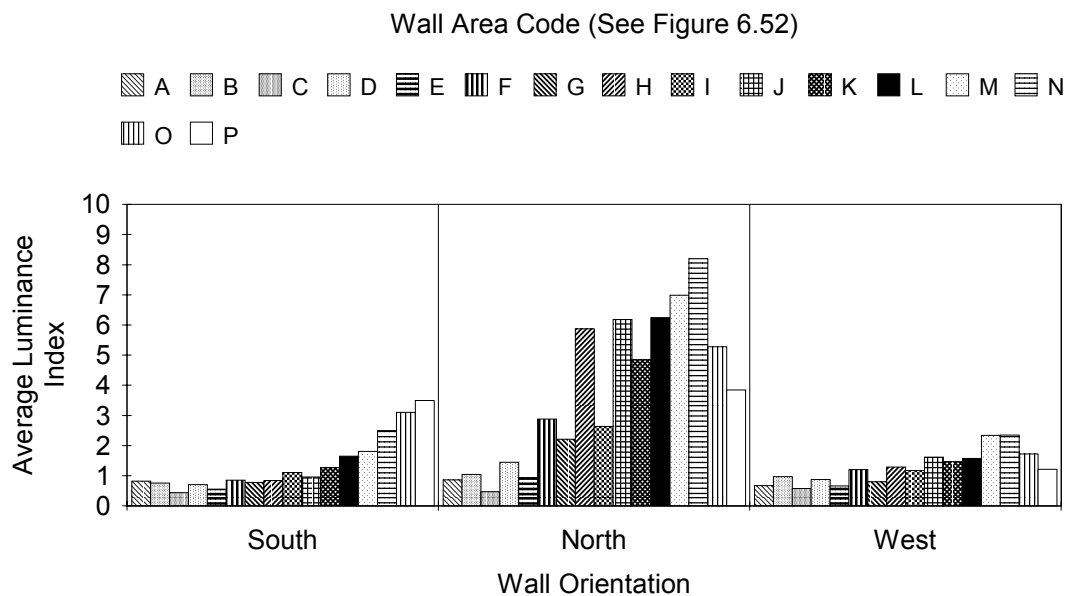


Figure 7.40 Average Sunlight Luminance Index Values for WI = 2.4 at Sun Alt. = 84.0° (Solar Noon, 6/21, Houston, TX)

TABLE 7.19  
Sunlight Luminance Ratios for WI = 0.6 without Canopy at Sun Alt. = 84.0°  
(Solar Noon, 6/21, Houston, TX)

Wall Area Code *	South Wall	North Wall	West Wall
A : B	1.0 : 1.3	1.0 : 1.8	1.0 : 1.4
B : C	1.5 : 1.0	1.6 : 1.0	1.8 : 1.0
C : D	1.0 : 1.7	1.0 : 2.5	1.0 : 1.5

TABLE 7.20  
Sunlight Luminance Ratios for WI = 1.2 without Canopy at Sun Alt. = 84.0°  
(Solar Noon, 6/21, Houston, TX)

Wall Area Code *	South Wall	North Wall	West Wall
A : B	1.3 : 1.0	1.0 : 1.5	1.0 : 1.6
B : C	1.0 : 1.0	1.5 : 1.0	1.7 : 1.0
C : D	1.0 : 1.4	1.0 : 2.3	1.0 : 1.7
D : E	1.3 : 1.0	1.4 : 1.0	1.8 : 1.0
E : F	1.0 : 1.2	1.0 : 2.4	1.0 : 2.2
F : G	1.0 : 1.1	1.7 : 1.0	1.8 : 1.0
G : H	1.0 : 1.9	1.0 : 2.3	1.0 : 1.2

TABLE 7.21  
 Sunlight Luminance Ratios for WI = 1.8 without Canopy at Sun Alt. = 84.0°  
 (Solar Noon, 6/21, Houston, TX)

Wall Area Code *	South Wall	North Wall	West Wall
A : B	1.0 : 1.6	1.0 : 1.2	1.0 : 1.7
B : C	2.2 : 1.0	1.4 : 1.0	1.8 : 1.0
C : D	1.0 : 1.3	1.0 : 2.2	1.0 : 1.6
D : E	1.2 : 1.0	1.8 : 1.0	1.6 : 1.0
E : F	1.0 : 1.5	1.0 : 2.9	1.0 : 2.1
F : G	1.3 : 1.0	1.9 : 1.0	1.9 : 1.0
G : H	1.0 : 1.4	1.0 : 4.1	1.0 : 2.1
H : I	1.1 : 1.0	3.2 : 1.0	1.7 : 1.0
I : J	1.0 : 1.3	1.0 : 3.9	1.0 : 1.9
J : K	1.0 : 1.1	1.0 : 1.0	1.7 : 1.0
K : L	1.0 : 1.2	1.0 : 1.1	1.0 : 1.1

TABLE 7.22  
Sunlight Luminance Ratios for WI = 2.4 without Canopy at Sun Alt. = 84.0°  
(Solar Noon, 6/21, Houston, TX)

Wall Area Code *	South Wall	North Wall	West Wall
A : B	1.1 : 1.0	1.0 : 1.2	1.0 : 1.4
B : C	1.7 : 1.0	2.2 : 1.0	1.7 : 1.0
C : D	1.0 : 1.6	1.0 : 3.1	1.0 : 1.5
D : E	1.3 : 1.0	1.5 : 1.0	1.3 : 1.0
E : F	1.0 : 1.5	1.0 : 3.1	1.0 : 1.8
F : G	1.1 : 1.0	1.3 : 1.0	1.5 : 1.0
G : H	1.0 : 1.1	1.0 : 2.7	1.0 : 1.6
H : I	1.0 : 1.3	2.2 : 1.0	1.1 : 1.0
I : J	1.2 : 1.0	1.0 : 2.3	1.0 : 1.4
J : K	1.0 : 1.3	1.3 : 1.0	1.1 : 1.0
K : L	1.0 : 1.3	1.0 : 1.3	1.0 : 1.1
L : M	1.0 : 1.1	1.0 : 1.1	1.0 : 1.5
M : N	1.0 : 1.4	1.0 : 1.2	1.0 : 1.0
N : O	1.0 : 1.2	1.6 : 1.0	1.4 : 1.0
O : P	1.0 : 1.1	1.4 : 1.0	1.0 : 1.4

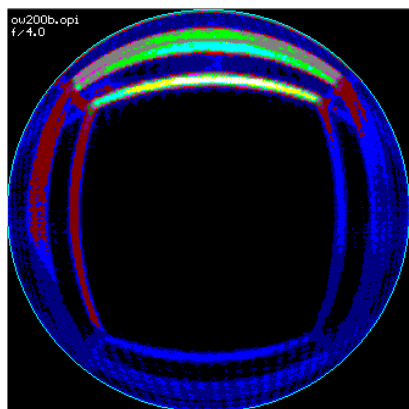
The video images in Figure 7.41 show the luminance distribution maps in four different atria without canopy at sun altitude angle of  $31.3^\circ$  which represents the noon sun on December 21 in Oklahoma City, OK. When the sun is at the low altitude, for all WI values the floor positions were completely shaded by the atrium well structures. At this condition, the sunlight illuminances discussed in the previous sections were due to the reflected sunlight from the atrium wall surfaces. In the images, the bright areas of the north wall were notable. It was also revealed that, at the lowest WI value (0.6), the average luminance condition on the side walls was higher than that of the south wall. However, as the WI increased the south wall showed slightly higher luminances than the two side walls.

A more notable phenomenon at this low sun altitude angle was the large differences in luminances between the solid walls and the windows. This was because the incident angles on the window areas were small, so that no specular reflections occurred on the glass surfaces, while the low incident angles on the vertical solid wall areas which were exposed to the sun received high-intensity sunlight.

Another interesting observation was the sunlight illuminance levels measured at the center floor position. As shown in Figure 7.42, at 0.6 WI the measured illuminance level was 97 lux. Then, it increased to 125 lux at 1.2 WI. At 1.8 and 2.4 WI values the illuminance levels decreased to 42 lux and 17 lux, respectively. Since the illuminance level at the floor position with this condition was provided only by the wall surfaces, the geometric relationship between the floor position and the high-luminance wall surfaces caused the different illuminance levels. It can be said that, among the four different WI values, the 1.2 WI had the largest Configuration Factor (CF) viewed from the floor position.

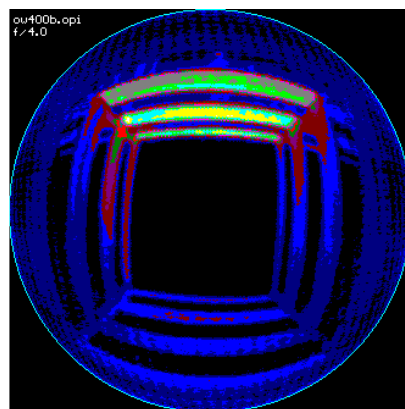
Figures 7.43 through 7.46 show the LI values at the four WI values. At a first glance, much increased LI values on the north wall can be found. Considering the concept of LI value, the high-luminance north wall greatly contributed to the measured illuminance levels.

Figures 7.47 through 7.50 show the average LI values on the wall areas on the three different walls. The Luminance Ratios between adjacent wall areas are presented in Tables 7.23 through 7.25. The figures and tables revealed that the Luminance Ratios between the bottom parts of the sunlit wall areas and window area just below the sunlit area always recorded maximum values. The highest LR value was observed at WI = 1.2 (atrium A4), which was 1 : 24.3 between the wall area C (window just below the sunlight area) and area D.



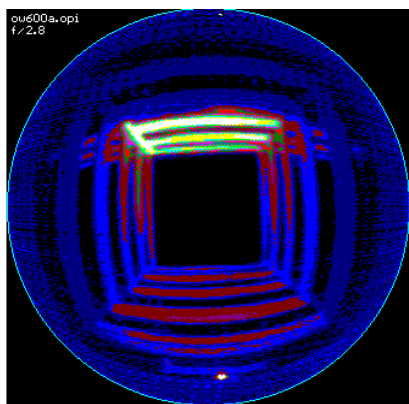
South

a. WI = 0.6 (Atrium A2, f/4)



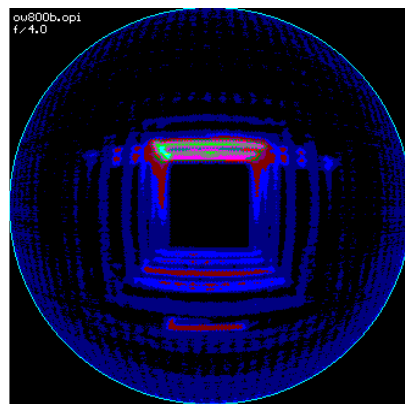
South

b. WI = 1.2 (Atrium A4, f/4)



South

c. WI = 1.8 (Atrium A6, f/2.8)



South

d. WI = 2.4 (Atrium A8, f/4)

Figure 7.41 Video Images of Sunlight Luminance Distributions without Canopy at Sun Alt. =  $31.3^\circ$  (Solar Noon, 12/21, Oklahoma City, OK)

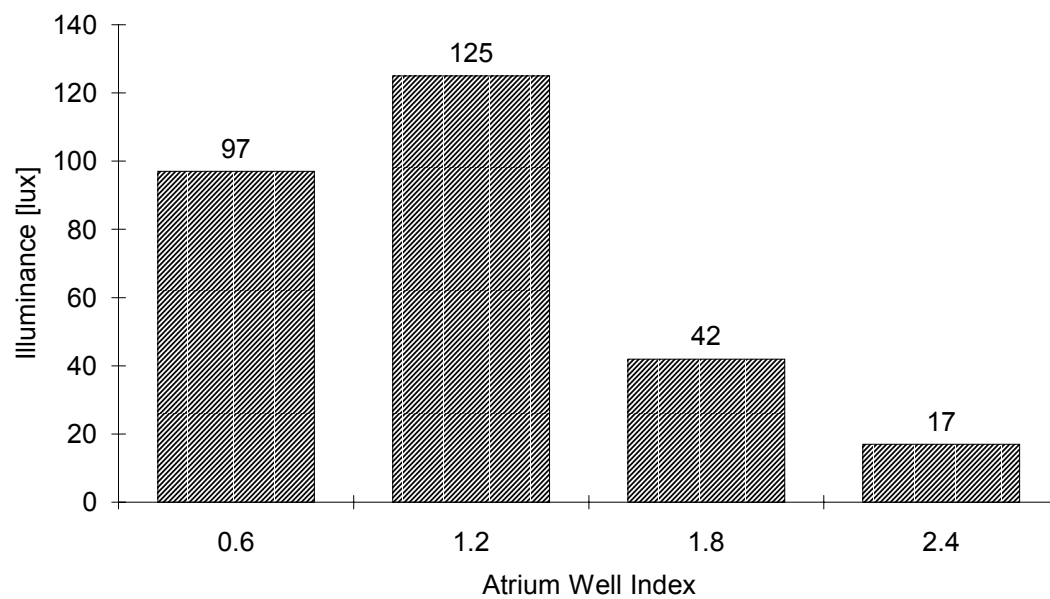


Figure 7.42 Sunlight Illuminance Levels Measured without Canopy at Sun Alt. =  $31.3^{\circ}$  (Solar Noon, 12/21, Oklahoma City, OK)

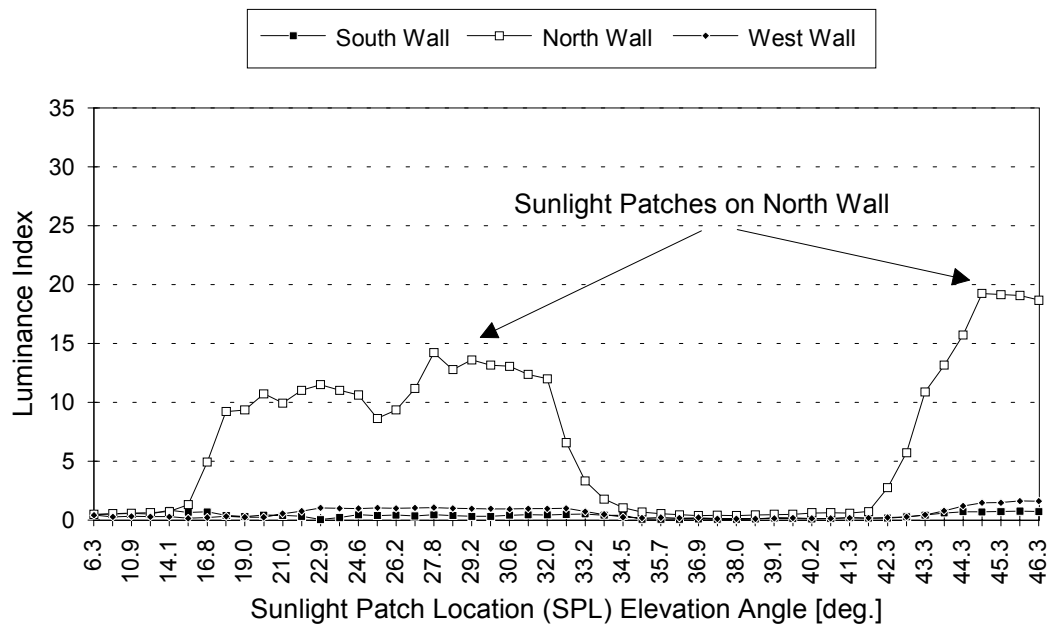


Figure 7.43 Sunlight Luminance Index Values for WI = 0.6 without Canopy at Sun Alt. = 31.3° (Solar Noon, 12/21, Oklahoma City, OK)

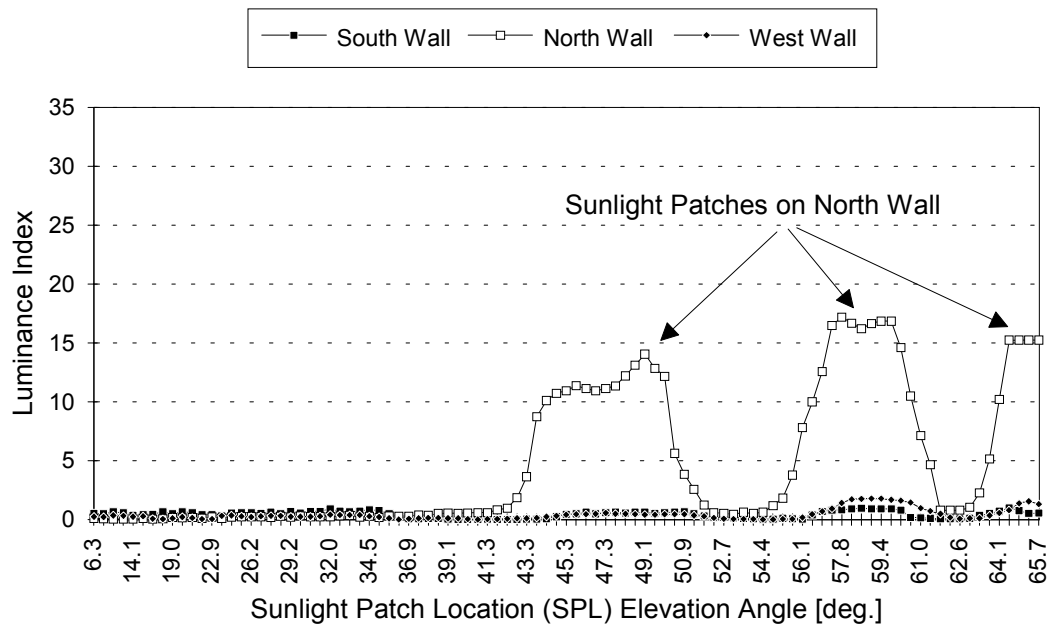


Figure 7.44 Sunlight Luminance Index Values for WI = 1.2 without Canopy at Sun Alt. = 31.3° (Solar Noon, 12/21, Oklahoma City, OK)



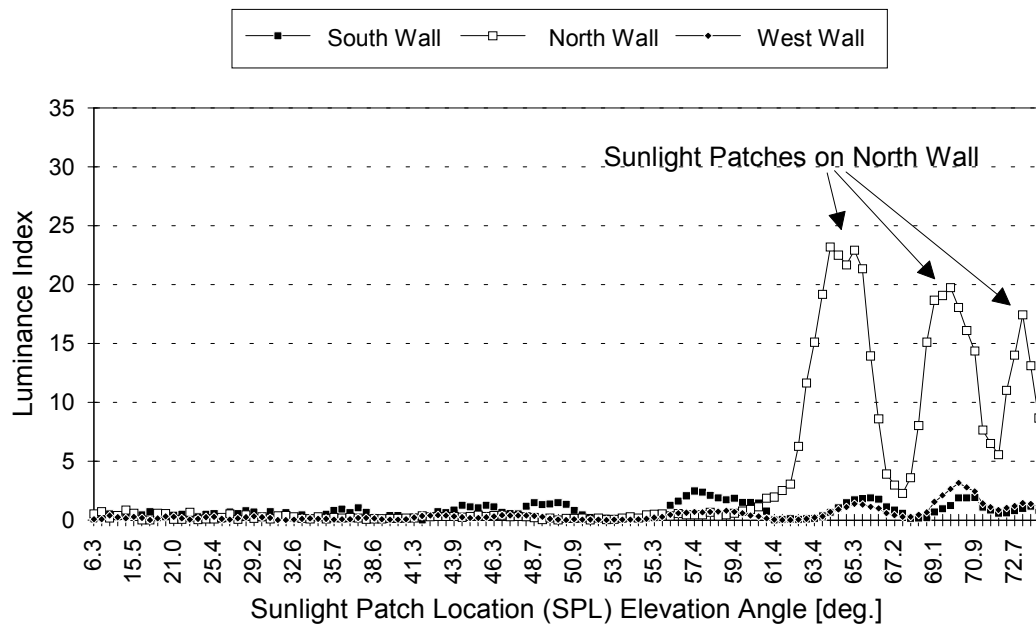


Figure 7.45 Sunlight Luminance Index Values for WI = 1.8 without Canopy at Sun Alt. = 31.3° (Solar Noon, 12/21, Oklahoma City, OK)

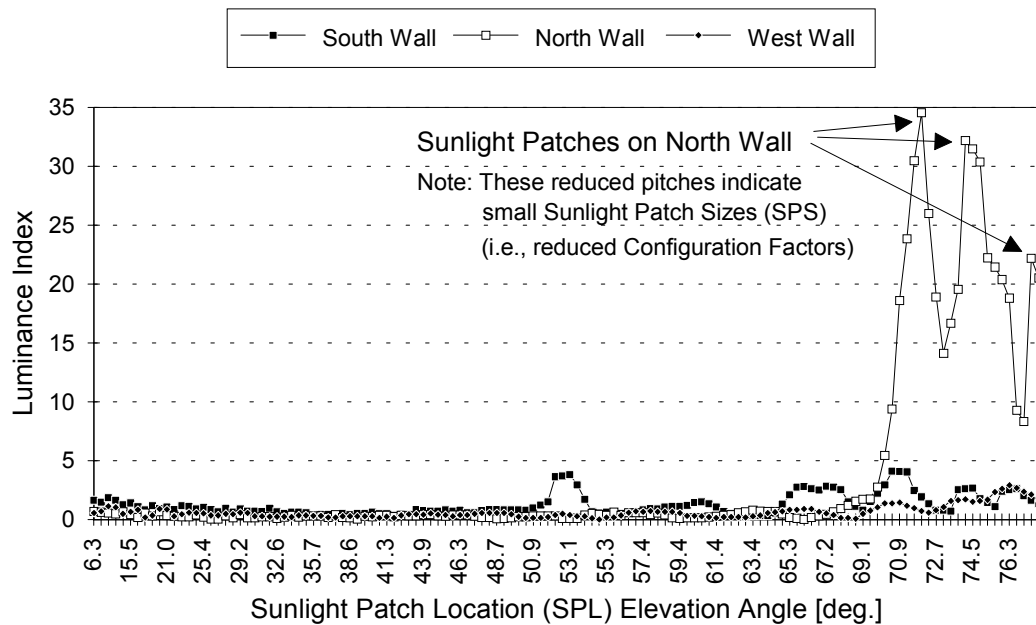


Figure 7.46 Sunlight Luminance Index Values for WI = 2.4 without Canopy at Sun Alt. = 31.3° (Solar Noon, 12/21, Oklahoma City, OK)

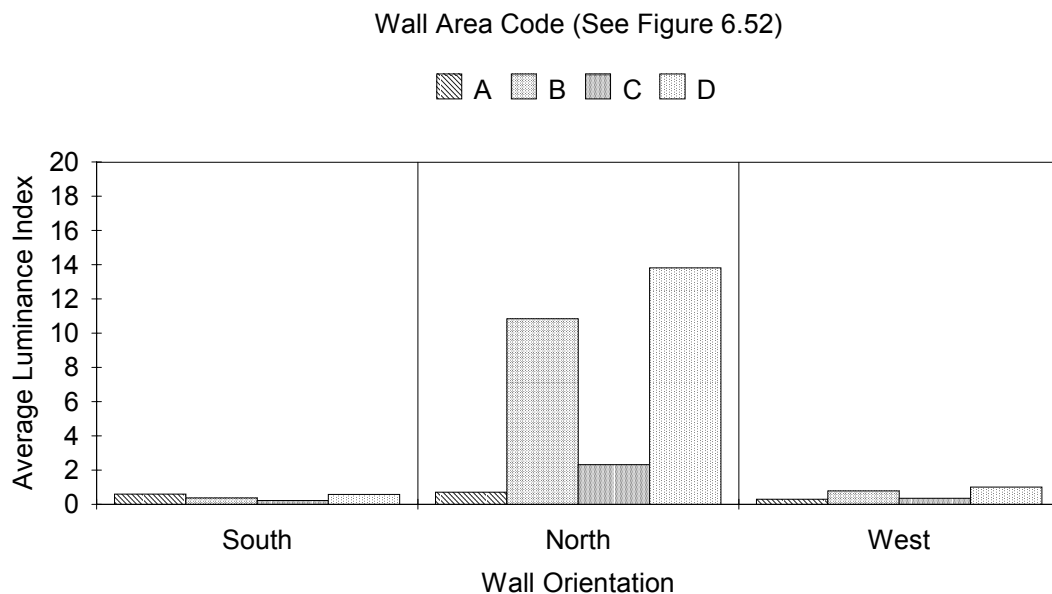


Figure 7.47 Average Sunlight Luminance Index Values for WI = 0.6 without Canopy at Sun Alt. = 31.3° (Solar Noon, 12/21, Okla. City, OK)

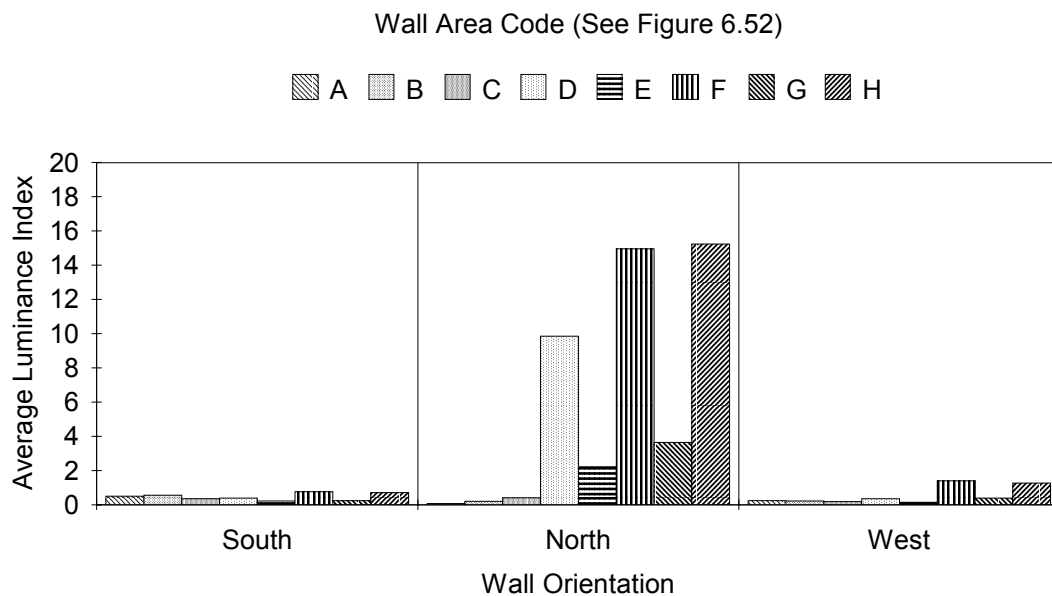


Figure 7.48 Average Sunlight Luminance Index Values for WI = 1.2 without Canopy at Sun Alt. = 31.3° (Solar Noon, 12/21, Okla. City, OK)

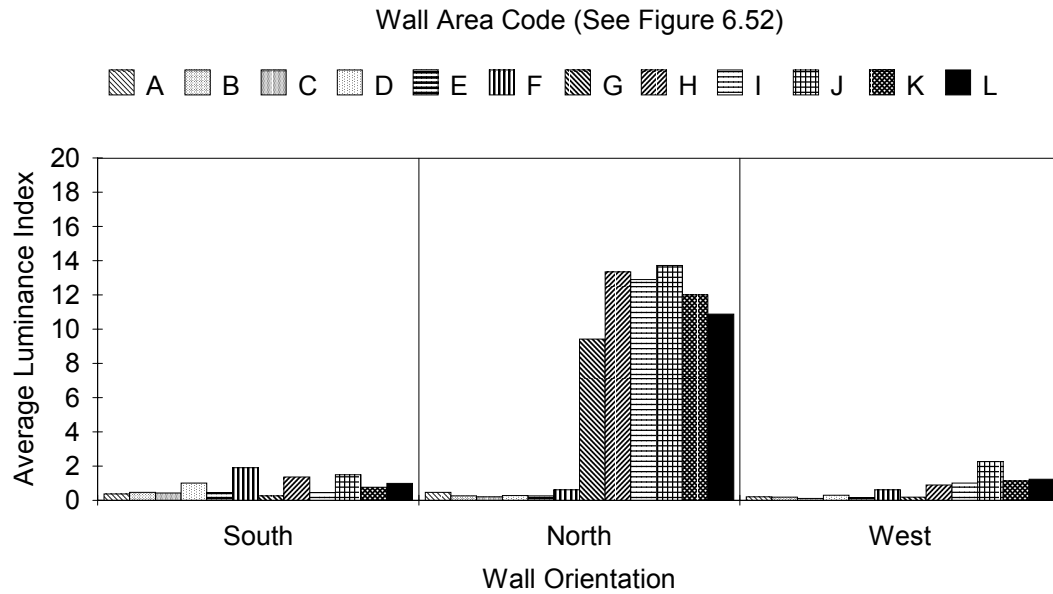


Figure 7.49 Average Sunlight Luminance Index Values for WI = 1.8 without Canopy at Sun Alt. = 31.3° (Solar Noon, 12/21, Okla. City, OK)

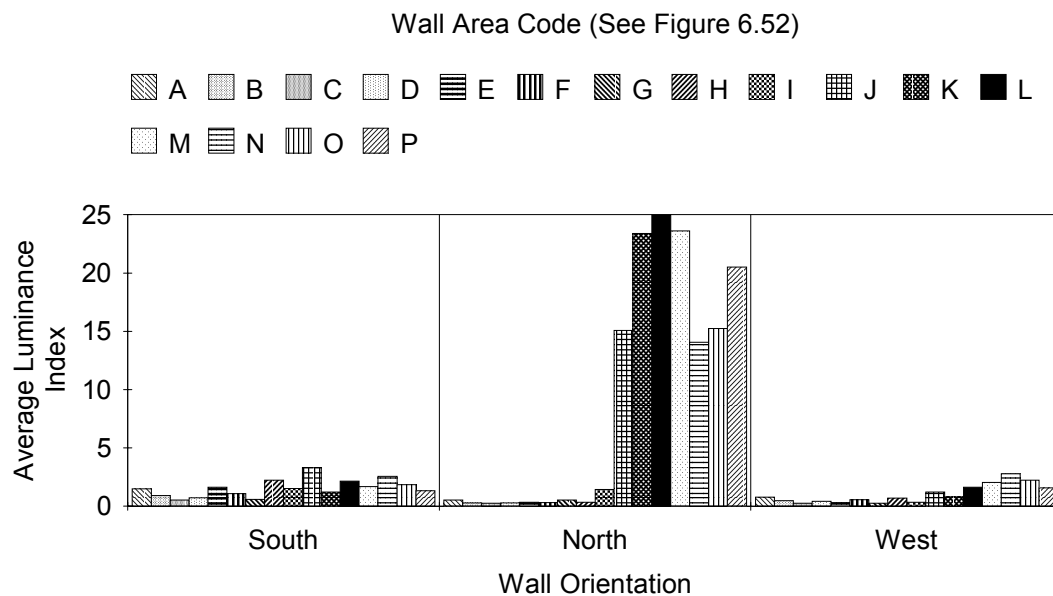


Figure 7.50 Average Sunlight Luminance Index Values for WI = 2.4 without Canopy at Sun Alt. = 31.3° (Solar Noon, 12/21, Okla. City, OK)

TABLE 7.23  
Sunlight Luminance Ratios for WI = 0.6 without Canopy at Sun Alt. = 31.3°  
(Solar Noon, 12/21, Oklahoma City, OK)

Wall Area Code *	South Wall	North Wall	West Wall
A : B	1.6 : 1.0	1.0 : 15.2	1.0 : 2.7
B : C	1.7 : 1.0	4.7 : 1.0	2.3 : 1.0
C : D	1.0 : 2.6	1.0 : 6.0	1.0 : 2.9

TABLE 7.24  
Sunlight Luminance Ratios for WI = 1.2 without Canopy at Sun Alt. = 31.3°  
(Solar Noon, 12/21, Oklahoma City, OK)

Wall Area Code *	South Wall	North Wall	West Wall
A : B	1.0 : 1.1	1.0 : 3.0	1.1 : 1.0
B : C	1.6 : 1.0	1.0 : 2.0	1.2 : 1.0
C : D	1.0 : 1.1	1.0 : 24.3	1.0 : 2.1
D : E	1.8 : 1.0	4.4 : 1.0	2.4 : 1.0
E : F	1.0 : 3.4	1.0 : 6.7	1.0 : 9.2
F : G	3.1 : 1.0	4.1 : 1.0	3.5 : 1.0
G : H	1.0 : 2.9	1.0 : 4.2	1.0 : 3.2

TABLE 7.25  
 Sunlight Luminance Ratios for WI = 1.8 without Canopy at Sun Alt. = 31.3°  
 (Solar Noon, 12/21, Oklahoma City, OK)

Wall Area Code *	South Wall	North Wall	West Wall
A : B	1.0 : 1.3	1.8 : 1.0	1.1 : 1.0
B : C	1.1 : 1.0	1.3 : 1.0	1.0 : 1.7
C : D	1.0 : 2.4	1.0 : 1.4	1.0 : 2.7
D : E	2.3 : 1.0	1.0 : 1.0	1.9 : 1.0
E : F	1.0 : 4.2	1.0 : 2.4	1.0 : 4.1
F : G	7.4 : 1.0	1.0 : 15.1	3.4 : 1.0
G : H	1.0 : 5.3	1.0 : 1.4	1.0 : 4.9
H : I	3.1 : 1.0	1.0 : 1.0	1.0 : 1.1
I : J	1.0 : 3.4	1.0 : 1.1	1.0 : 2.2
J : K	1.9 : 1.0	1.1 : 1.0	2.0 : 1.0
K : L	1.0 : 1.3	1.1 : 1.0	1.0 : 1.1

TABLE 7.26  
Sunlight Luminance Ratios for WI = 2.4 without Canopy at Sun Alt. = 31.3°  
(Solar Noon, 12/21, Oklahoma City, OK)

Wall Area Code *	South Wall	North Wall	West Wall
A : B	1.6 : 1.0	1.8 : 1.0	1.6 : 1.0
B : C	1.7 : 1.0	1.1 : 1.0	1.9 : 1.0
C : D	1.0 : 1.4	1.0 : 1.1	1.0 : 1.6
D : E	1.0 : 2.2	1.0 : 1.3	1.5 : 1.0
E : F	1.5 : 1.0	1.1 : 1.0	1.0 : 2.0
F : G	1.8 : 1.0	1.0 : 1.6	2.1 : 1.0
G : H	1.0 : 3.8	1.6 : 1.0	1.0 : 2.7
H : I	1.5 : 1.0	1.0 : 4.2	2.1 : 1.0
I : J	1.0 : 2.2	1.0 : 10.5	1.0 : 3.7
J : K	2.7 : 1.0	1.0 : 1.5	1.5 : 1.0
K : L	1.0 : 1.8	1.0 : 1.1	1.0 : 2.0
L : M	1.3 : 1.0	1.1 : 1.0	1.0 : 1.3
M : N	1.0 : 1.5	1.7 : 1.0	1.0 : 1.4
N : O	1.0 : 1.4	1.0 : 1.1	1.2 : 1.0
O : P	1.0 : 1.4	1.0 : 1.3	1.0 : 1.4

### 7.2.2 Sunlight Patches on Wall Areas with Canopies

As discussed in Chapter 2, the qualitative lighting objective in atria may be to create sparkle. This objective can be achieved by allowing some direct sunlight into the atrium space. In this section, the locations and sizes of sunlight patches on the atrium wall surfaces were investigated in terms of their elevation angles and percent coverage of corresponding wall area.

A total of 10 canopy systems were selected for this test. They included 2-unit and 4-unit sawtooth canopies with vertical apertures oriented to south (No. 04S and 08S) and north (No. 04N and 08N), 4-unit sawtooth canopies with 15° sloping apertures oriented to south (No. 13S) and north (No. 13N), 4-unit sawtooth canopies with 60° sloping apertures oriented to south (No. 16S) and north (No. 16N), pyramid skylight with tinted transparent glazing (No. 27), and waffle skylight with WWI = 0.5 and 85 % surface reflectance (No. 33). In addition, the pyramid skylight with white translucent glazing was tested for a comparison purpose even though it did not allow sunlight patches. The atrium WI values involved in this test were 0.6 (atrium A2), 1.2 (atrium A4), 1.8 (atrium A6) and 2.4 (atrium A8). The sun altitude angles were the same as those of the previous section (84.0° and 31.3°).

After completing the luminance mapping, all of the images were examined to see if any sunlight patches existed on the wall surfaces. During the image analysis procedure, images which were fully exposed to the artificial sun were excluded. Meanwhile, some of the images captured at the low sun altitude angle were too dark. However, the sunlight patches were readily noticeable owing to high contrast between the sunlight patches and the adjacent dark area. Since the current analysis deals with the geometric information of sunlight patches, those images were included.

The Sunlight Patch Locations (SPL) in terms of elevation angles and the Sunlight Patch Sizes (SPS) in terms of Configuration Factors (CF) on the north wall and the two side walls were determined by the thresholding algorithm of the image analysis software which was discussed in Chapter 3. Then, to calculate the percent coverage of the sunlight patch areas on each wall, the sum of SPS were divided by the CF value of a corresponding wall. Since, the video images were captured at the center floor position, the CF values of four walls were the same at a given WI value. Figure 7.51 shows the geometric relationship between the center floor position and a vertical wall for which the CF value of the vertical wall can be calculated by Equation 7.1 (Hopkinson et al. 1966, p.

90). Table 7.27 shows the calculated CF values of the vertical walls at the four different WI values.

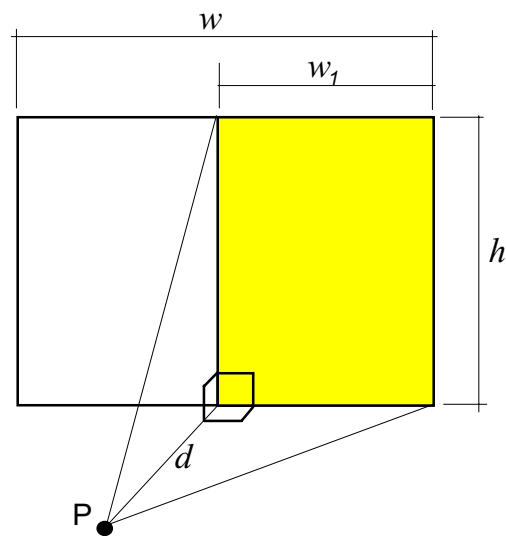


Figure 7.51 Geometric Relationship between Point P and Vertical Wall to Calculate Configuration Factor

$$CF_{wall} = \frac{1}{2\pi} \left( \tan^{-1} \frac{w_1}{d} - \frac{d}{\sqrt{h^2 + d^2}} \tan^{-1} \frac{w_1}{\sqrt{h^2 + d^2}} \right) \times 2 \quad (7.1)$$

TABLE 7.27  
Configuration Factors (CF) of Vertical Walls (1/2 in. = 1 ft Scale)

Well Index	h (in. / ft)	w <sub>1</sub> (in. / ft)	d (in. / ft)	CF <sub>wall</sub>
0.6	10.5 / 21	10 / 20	10 / 20	0.1175
1.2	22.5 / 45	10 / 20	10 / 20	0.2001
1.8	34.5 / 69	10 / 20	10 / 20	0.2259
2.4	46.5 / 93	10 / 20	10 / 20	0.2361

Tables 7.28 and 7.29 summarize the results of the image analysis for the two sun altitude angles. Figures 7.52 through 7.57 show the video images with segmented sunlight patches processed by the image analysis software.



TABLE 7.28  
Sunlight Patch Locations (SPL) and Sunlight Patch Sizes (SPS) on Wall Areas with  
Canopies at Sun Alt. = 84.0° (Solar Noon, 6/21, Houston, TX)

CC	WI = 0.6	WI = 1.2	WI = 1.8	WI = 2.4
04S	None	E&W: 46°-58° 0.0039 (1.9 %)	E&W: 42°-73° 0.0077 (3.4 %) N: 50°-73° 0.0051(2.3 %)	E&W: 40°-72° 0.0108 (4.6 %) N: 60°-72° 0.0077 (3.3 %)
04N	None	None	None	None
08S	None	E&W: 46°-58° 0.0234 (11.7 %) N: 52°-59° 0.0127 (6.3 %)	E&W: 45°-73° 0.0203 (9.0 %) N: 41°-49° 0.0344 (15.2 %)	None
08N	None	None	None	None
13S	E&W: 21°-31° 0.0186 (15.8 %)	Full sun	Full sun	Full sun
13N	Full sun	E&W: 17°-66° 0.0245 (12.2 %) N: 56°-66° 0.0399 (19.9 %)	E&W: 17°-73° 0.0297 (13.1 %) N: 16°-45° 0.0572 (25.3 %)	E&W: 21°-77° 0.0552 (23.4 %) N: 43°-77° 0.0876 (37.1 %)
16S	E&W: 23°-26° 0.0047 (4.0 %)	E&W: 17°-66° 0.0129 (6.4 %)	Full sun	Full sun
16N	E&W: 23°-26° 0.0026 (2.2 %)	E&W: 17°-66° 0.0108 (5.4 %)	Full sun	Full sun
27	Full sun	Full sun	Full sun	Full sun
33	Full sun	Full sun	Full sun	Full sun

where CC = Canopy Code (See Table 4.8)

E&W = average of east and west wall totals

N = north wall total

TABLE 7.29  
Sunlight Patch Locations (SPL) and Sunlight Patch Sizes (SPS) on Wall Areas with  
Canopies at Sun Alt. = 31.3° (Solar Noon, 12/21, Oklahoma City, OK)

CC	WI = 0.6	WI = 1.2	WI = 1.8	WI = 2.4
04S	N: 26°-55° 0.0428 (36.4 %)	N: 47°-61° 0.0360 (18.0 %)	N: 64°-71° 0.0194 (8.6 %)	N: 72°-75° 0.0073 (3.1 %)
04N	None	None	None	None
08S	N: 30°-54° 0.0290 (24.7 %)	N: 48°-53° 0.0211(10.5 %)	N: 64°-66° 0.0107 (4.7 %)	N: 72°-73° 0.0038 (1.6 %)
08N	None	None	None	None
13S	N: 24°-50° 0.0561 (47.7 %)	N: 47°-67° 0.0435 (21.7 %)	N: 64°-65° 0.0081(3.6 %)	N: 71°-77° 0.0180 (7.6 %)
13N	N: 31°-54° 0.0199 (16.9 %)	N: 59°-61° 0.0059 (2.9 %)	None	None
16S	N: 26°-50° 0.0569 (48.4 %)	N: 48°-67° 0.0412 (20.6 %)	N: 64°-70° 0.0174 (7.7 %)	N: 71°-76° 0.0168 (7.1 %)
16N	None	None	None	None
27	N: 26°-50° 0.0552 (47.0 %)	N: 46°-67° 0.0335 (16.7 %)	N: 63°-73° 0.0195 (8.6 %)	N: 71°-76° 0.0175 (7.4 %)
33	N: 27°-35° 0.0160 (13.6%)	N: 46°-62° 0.0209 (10.4 %)	N: 63°-70° 0.0099 (4.4 %)	N: 71°-72° 0.0052 (2.2 %)

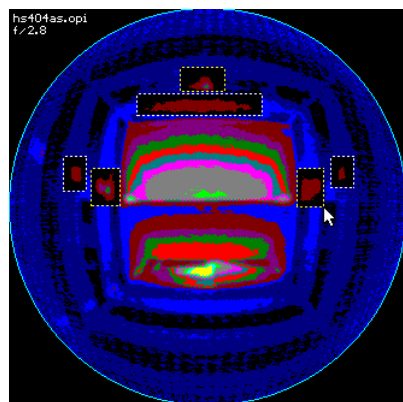
where CC = Canopy Code (See Table 4.8)

N = north wall total

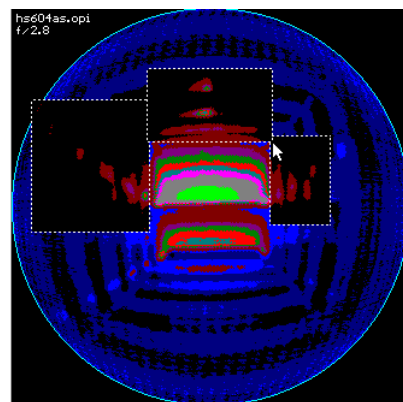
The video images in Figures 7.52 and 7.53 show that the sawtooth canopies with south-facing vertical apertures caused horizontally long areas of sunlight patches on the north wall at the low sun altitude angle. The elevation angles of the sunlight patches with the sawtooth canopies 04S and 08S on the north wall were between  $47^\circ$  and  $61^\circ$ . Since the far field view angle of the human eye is  $60^\circ$  above and below the horizon (Stein and Reynolds 1992, p. 929), those sunlight patches could be readily visible to people at normal viewing positions. However, as the WI increased the relative sizes decreased and the elevation angle increased. At WI = 1.8, the elevation angles were between  $64^\circ$  and  $71^\circ$  and at WI = 2.4, they were  $72^\circ$  and  $75^\circ$ . These elevation angles are off-boundary of the normal view field, but they could be visible by moving the eye or the head to upward.

As shown in Table 7.29, at WI = 0.6, the percent coverages of the sunlight patch areas were 47.7 % with canopy 13S, 48.4 % with canopy 16S, and 47.0 % with canopy 27. If these numbers are compared with the result of the previous study (Boubekri et al. 1991), which found the size of sunlight patch area from 15 % to 25 % of total floor area as optimal and 40 % as maximum for occupants' environmental satisfaction, it exceeded the maximum allowable value. However, the previous work was about office environment where serious paper works were involved. Considering that most of the visual tasks in building lobby area are usually casual, because atrium spaces are usually used as lobbies, it might not be concluded that the large sunlight patch area functioned against occupants' visual pleasure. Even though a detailed discussion about psycho-biological effects of luminous environment is out of scope of this study, it might be a logical extension of this analysis to investigate the relationship between the sizes and locations of sunlight patch areas and the occupants' visual satisfactions in spaces for casual visual tasks for future study.

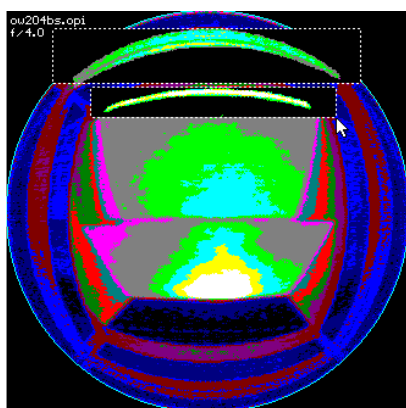
Meanwhile, as indicated in Figures 7.54 and 7.55, the sawtooth canopies with sloping apertures created the same types of sunlight patches on the north wall at the low sun angle, but they created visually interesting rectangular segmented sunlight patches on the two side walls at the high sun. As indicated in the images numbered "e" and "f" in Figures 7.54 and 7.55, owing to the high sun altitude angle, the sunlight patches existed from the top area to the bottom area of the two side walls. The images revealed that during the image capture, the location of the artificial sun was a little bit deviated from the south, because the sunlight patches on the east and the west walls were not symmetrical. However, those images were good enough to demonstrate the character of this type of sawtooth canopies. Figure 7.56 shows the photo of sunlight patches on the west wall created by the sawtooth canopy (No. 13N) at sun altitude angle of  $84^\circ$ .



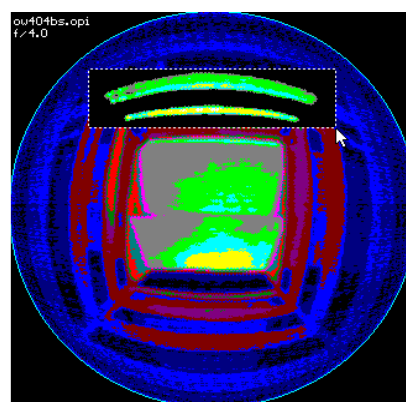
a. WI = 1.2, Sun Alt. = 84.0°



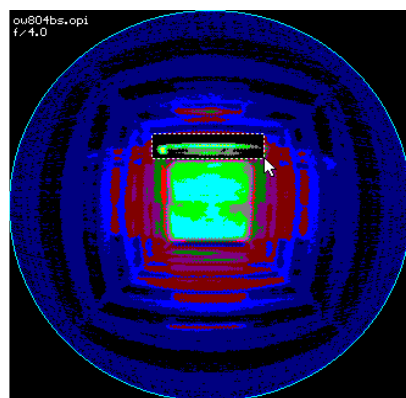
b. WI = 1.8, Sun Alt. = 84.0°



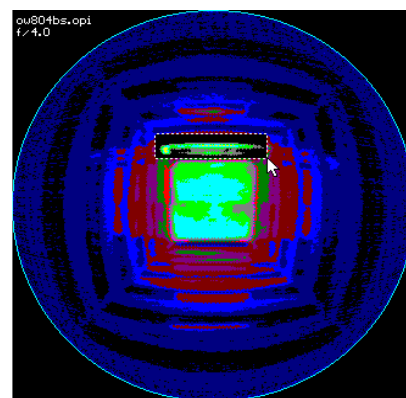
c. WI = 0.6, Sun Alt. = 31.3°



d. WI = 1.2, Sun Alt. = 31.3°

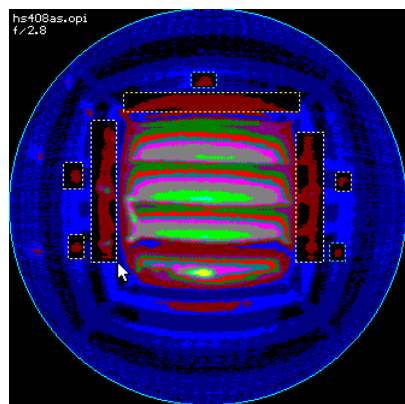


e. WI = 1.8, Sun Alt. = 31.3°

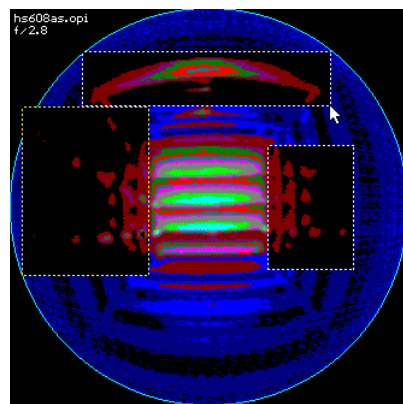


f. WI = 2.4, Sun Alt. = 31.3°

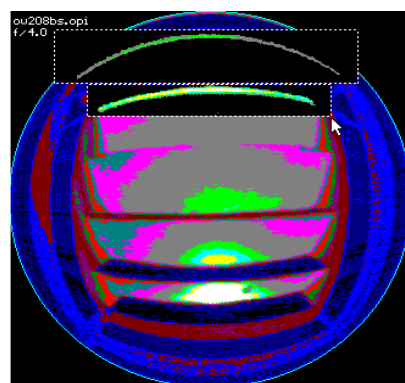
Figure 7.52 Sunlight Patches with Sawtooth Canopy 04 Facing South (North is up, See Table 4.8 for Canopy Code)



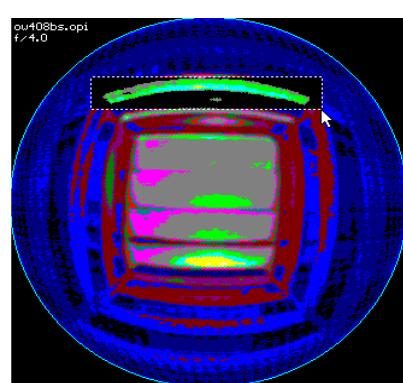
a. WI = 1.2, Sun Alt. = 84.0°



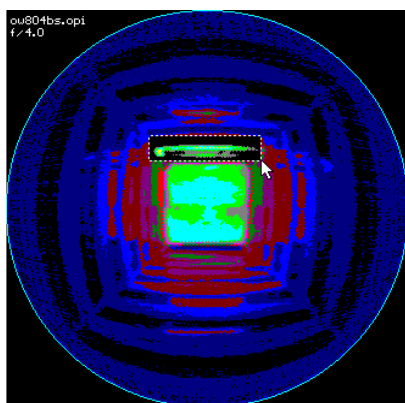
b. WI = 1.8, Sun Alt. = 84.0°



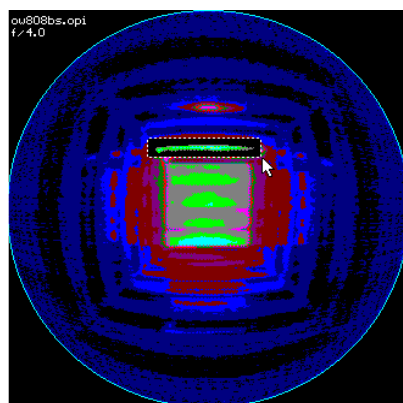
c. WI = 0.6, Sun Alt. = 31.3°



d. WI = 1.2, Sun Alt. = 31.3°

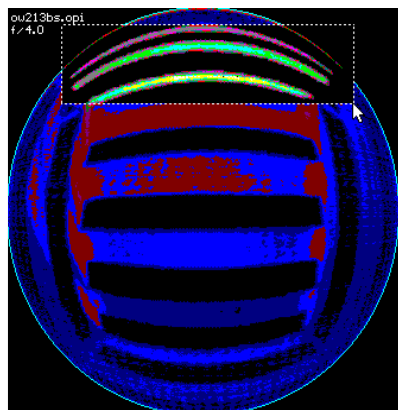


e. WI = 1.8, Sun Alt. = 31.3°

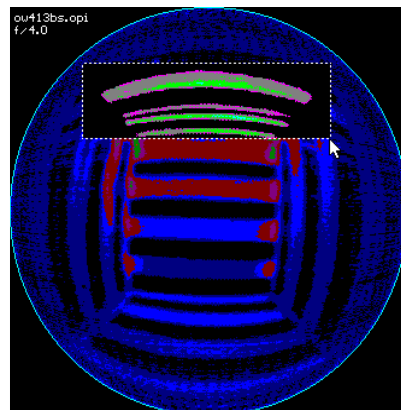


f. WI = 2.4, Sun Alt. = 31.3°

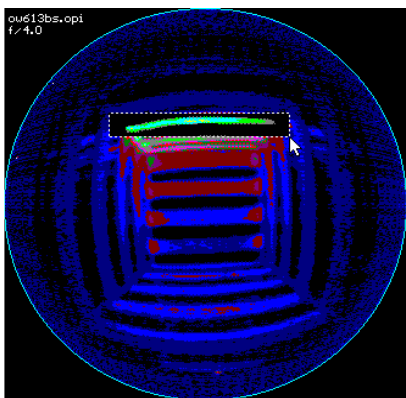
Figure 7.53 Sunlight Patches with Sawtooth Canopy 08 Facing South (North is up, See Table 4.8 for Canopy Code)



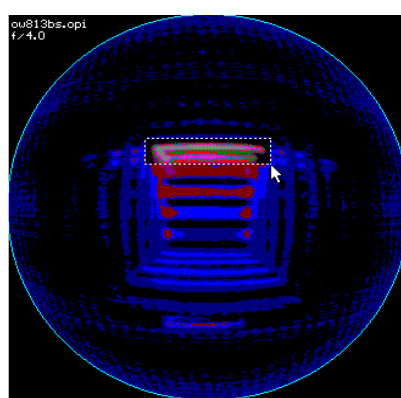
a. No. 13S (WI = 0.6, Sun Alt. = 31.3°)



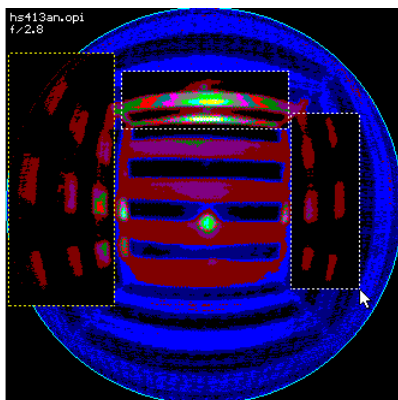
b. No. 13S (WI = 1.2, Sun Alt. = 31.3°)



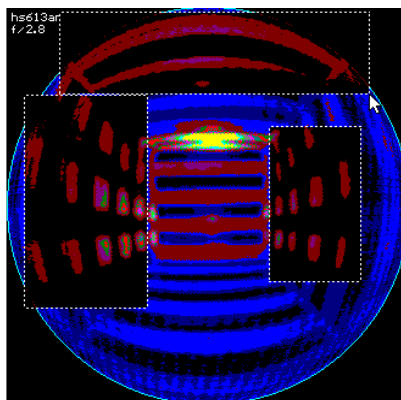
c. No. 13S (WI = 1.8, Sun Alt. = 31.3°)



d. No. 13S (WI = 2.4, Sun Alt. = 31.3°)

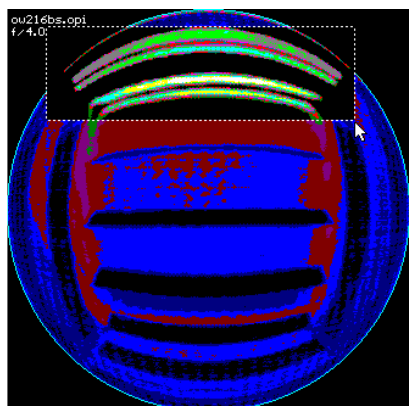


e. No. 13N (WI = 1.2, Sun Alt. = 84.0°)

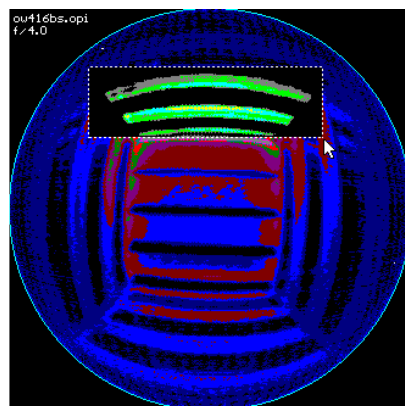


f. No. 13N (WI = 1.8, Sun Alt. = 84.0°)

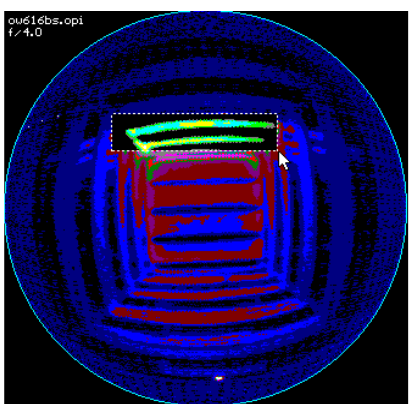
Figure 7.54 Sunlight Patches with Sawtooth Canopies 13S and 13N  
(North is up, See Table 4.8 for Canopy Code)



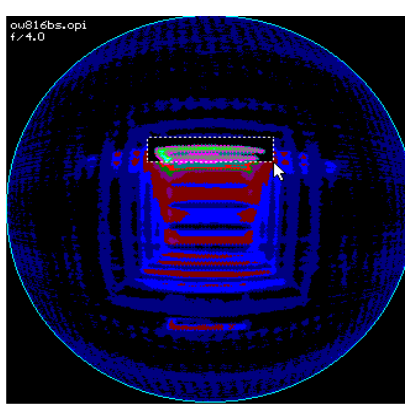
a. No. 16S (WI = 0.6, Sun Alt. = 31.3°)



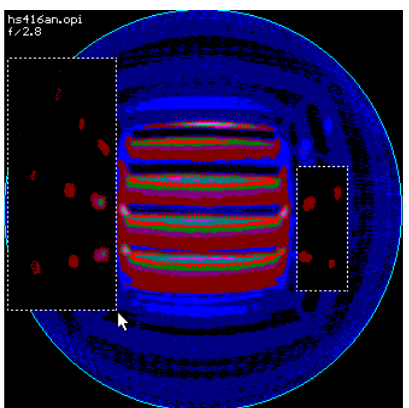
b. No. 16S (WI = 1.2, Sun Alt. = 31.3°)



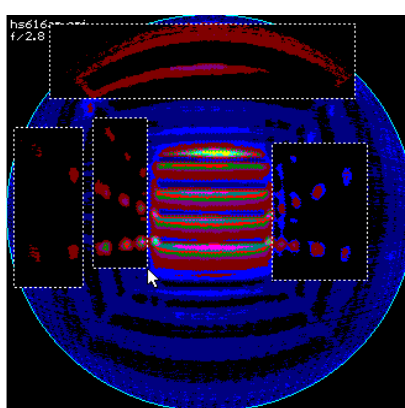
c. No. 16S (WI = 1.8, Sun Alt. = 31.3°)



d. No. 16S (WI = 2.4, Sun Alt. = 31.3°)



c. No. 16N (WI = 1.2, Sun Alt. = 84.0°)



d. No. 16N (WI = 1.8, Sun Alt. = 31.3°)

Figure 7.55 Sunlight Patches with Sawtooth Canopies 16S and 16N  
(North is up, See Table 4.8 for Canopy Code)

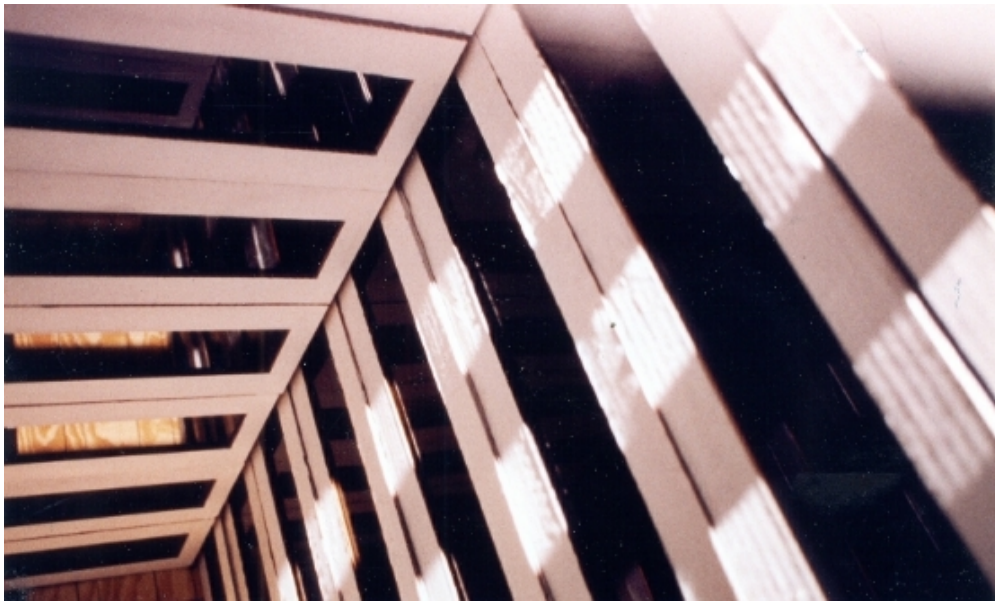


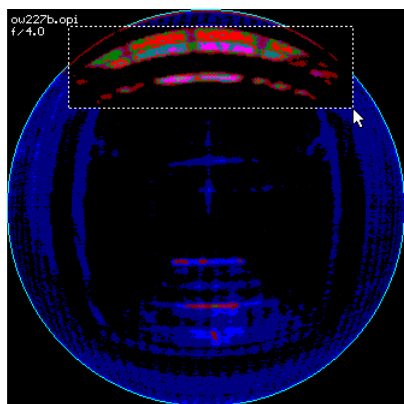
Figure 7.56 Photo of Sunlight Patches on West Wall Created by Sawtooth Canopy 13N at WI = 2.4 (Atrium A8, Sun Alt. = 84°)  
(See Table 4.8 for Canopy Code)



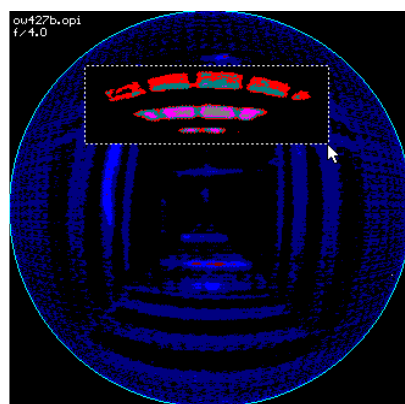
The video images in Figures 7.57 and 7.58 demonstrate that the pyramid skylight and waffle skylight also created interesting sunlight patches on the north wall due to the patterns of the opaque structural members. Especially, Figure 7.57 demonstrates the completely different roles of the glazing materials with different transparency. In terms of light diffusion which reduces glare problems, the translucent glazing material works better. However, if the visually interesting sparkles are the primary concern, the transparent glazing material works better. To accommodate these two conflicting design requirements, combining the two different glazing materials with different portions in areas on a given canopy system can be a design choice.

From this analysis, it was learned that the sizes and locations of sunlight patches were purely dependent upon the geometric relationship among wall orientation, canopy aperture, and the sun. In addition, the major spatial patterns of sunlight patches were primarily decided by the geometric patterns of the solid wall and window glass areas (see the video images "e" and "f" in Figures 7.54 and 7.55) and the sub-patterns were decided by the geometric feature of the structural members of canopy systems (see the video images in Figures 7.57 and 7.58).

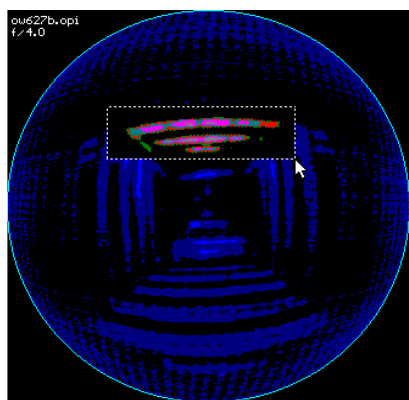
A tentative conclusion made from this video image analysis was that the skylight type canopies with transparent glazing transmitted too much direct sunlight in a hot climatic zone which would increase the thermal conditioning load. Instead, the sawtooth canopies with vertical apertures effectively blocked the direct beam sunlight, while they created visually pleasing sunlight patches on the side walls.



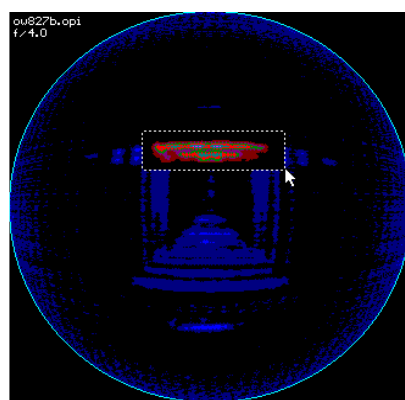
a. No. 27 (WI = 0.6, Sun Alt. = 31.3°)



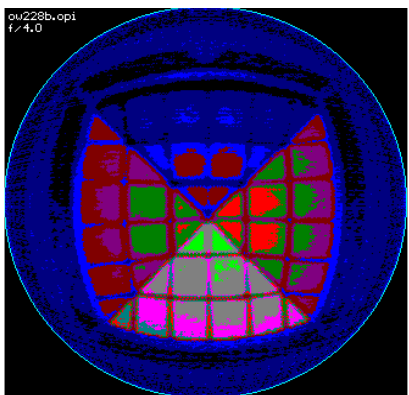
b. No. 27 (WI = 1.2, Sun Alt. = 31.3°)



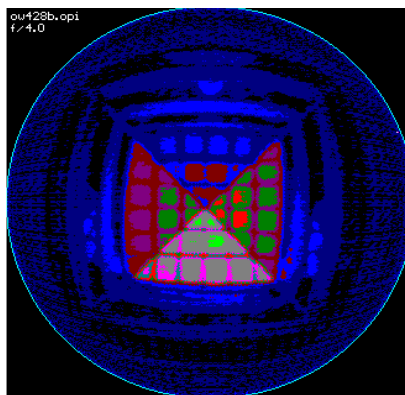
c. No. 27 (WI = 1.8, Sun Alt. = 31.3°)



d. No. 27 (WI = 2.4, Sun Alt. = 31.3°)

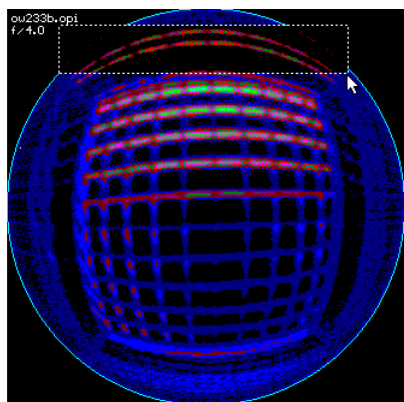


e. No. 28 (WI = 0.6, Sun Alt. = 31.3°)

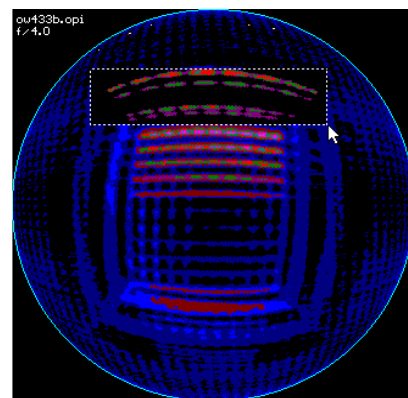


f. No. 28 (WI = 1.2, Sun Alt. = 31.3°)

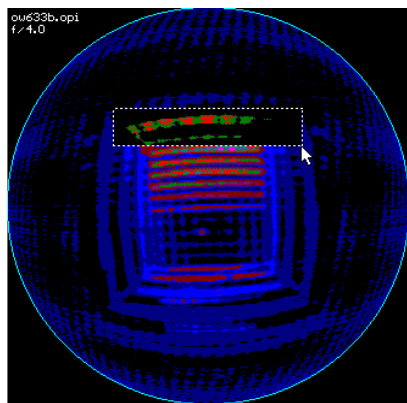
Figure 7.57 Sunlight Patches with Pyramid Skylights 27 and 28  
(North is up, See Table 4.8 for Canopy Code)



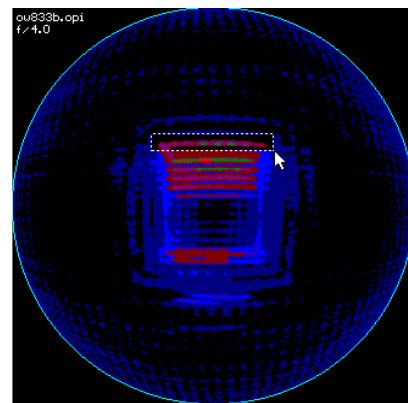
a. WI = 0.6, Sun Alt. =  $31.3^\circ$



b. WI = 1.2, Sun Alt. =  $31.3^\circ$



c. WI = 1.8, Sun Alt. =  $31.3^\circ$



d. WI = 2.4, Sun Alt. =  $31.3^\circ$

Figure 7.58 Sunlight Patches with Waffle Skylight 33 (WWI = 0.5)  
(North is up, See Table 4.8 for Canopy Code)